Environmental and Sustainability Indicators 24 (2024) 100511

Contents lists available at ScienceDirect

Environmental and Sustainability Indicators

journal homepage: www.sciencedirect.com/journal/environmental-and-sustainability-indicators

Marine microbial community taxonomic and functional indicators to volcanic and anthropogenic stressors in Deception Island, Antarctica

Bernardo Duarte [a,b,*], Ana Cruz-Silva [b,c], Eduardo Feijão [a,c], Marcelo Pereira [c], Mónica Nunes [c], Andreia Figueiredo [b,c], Ana Rita Matos [b,c], Ricardo Dias [c,d], Vanessa Fonseca [b,e], Carla Gameiro [f], Maria Teresa Cabrita [g,h]

[a] MARE - Marine and Environmental Sciences Centre & ARNET – Aquatic Research Network Associated Laboratory, Faculdade de Ciências da Universidade de Lisboa, Campo Grande, 1749-016, Lisboa, Portugal
[b] Departamento de Biologia Vegetal da Faculdade de Ciências da Universidade de Lisboa, Campo Grande, 1749-016, Lisboa, Portugal
[c] BioISI—Instituto de Biossistemas e Ciências Integrativas, Departamento de Biologia Vegetal, Faculdade de Ciências da Universidade de Lisboa, Campo Grande, 1749-016, Lisboa, Portugal
[d] cE3c—Center for Ecology, Evolution and Environmental Changes & CHANGE—Global Change and Sustainability Institute, Faculdade de Ciências da Universidade de Lisboa, Campo Grande, 1749-016, Lisboa, Portugal
[e] Departamento de Biologia Animal da Faculdade de Ciências da Universidade de Lisboa, Campo Grande, 1749-016, Lisboa, Portugal
[f] IPMA - Instituto Português do Mar e da Atmosfera - Divisão de Modelação e Recursos de Pesca (DivRP), Av. Dr. Alfredo Magalhães Ramalho, 1495-165, Algés, Portugal
[g] Centro de Estudos Geográficos (CEG), Instituto de Geografia e Ordenamento do Território (IGOT), Universidade de Lisboa, Rua Branca Edmée Marques, 1600-276, Lisboa, Portugal
[h] Laboratório Associado Terra, Portugal

ARTICLE INFO

Keywords:
Prokaryome
Virome
Functional traits
Resistome
Anthropogenic pressures
Polar microbiomes

ABSTRACT

In recent years, the growth in Antarctic tourism has stimulated research on the anthropogenic impacts on the region, boosted by advances in OMIC technologies applied to polar microbial communities. This study aimed to assess the human impacts on marine prokaryotic and viral communities of Deception Island by identifying potential taxonomic, functional, and resistome indicators of both anthropogenic and natural/volcanic pressures. Proteobacteria, Bacteroidetes, and Actinobacteria were the dominant phyla, with notable variations attributed to volcanic activity and anthropogenic pressure. The abundance of Euryarchaeota in regions with increased volcanic activity underlines their adaptability to extreme conditions. Their mercury resistance coupled with their ability to cope with toxic heavy metals is a critical component in managing volcanic mercury concentrations. Actinobacteria, Cyanobacteria, Planctomycetes, and Synergistetes showed distinctive abundance patterns with potential ecological implications related to volcanic environments. Functional analyses revealed the enrichment of functions associated with metal-based, hydrocarbon degradation, and nitrogen metabolism. Submarine volcanic vents contributed significantly to the shape of functional diversity. Identification of specific functions related to nosocomial infections and gastroenteritis highlights the impact of anthropogenic activities on functional traits. Antibiotic resistance genes (ARGs) showed nuanced patterns influenced by both anthropogenic pressure and volcanic activity. Actinobacteria were correlated with increased ARG abundance, which was enhanced by wastewater disposal. Remarkably, Fumarole Bay showed an increased prevalence of certain ARGs, despite a lower anthropogenic impact, suggesting a unique selective pressure induced by volcanic activity. The responsiveness of these indicators to varying levels of pressure characterizes them as valuable tools for assessing and mitigating anthropogenic impacts on the marine waters of Deception Island.

1. Introduction

Autogenic and allogenic alterations have changed ecosystems worldwide (Arroyo-Rodríguez et al., 2017; Bisht et al., 2023b). Autogenic changes, such as the advancement of successional stages, lead to dynamic equilibrium characterized by pre-climax and climax

* Corresponding author. MARE - Marine and Environmental Sciences Centre & ARNET – Aquatic Research Network Associated Laboratory, Faculdade de Ciências da Universidade de Lisboa, Campo Grande, 1749-016, Lisboa, Portugal.
E-mail address: baduarte@fc.ul.pt (B. Duarte).

https://doi.org/10.1016/j.indic.2024.100511
Received 2 August 2024; Received in revised form 10 October 2024; Accepted 14 October 2024
Available online 16 October 2024

conditions, whereas allogenic changes cause stress in the ecosystem and result in retrogressive changes (Bisht et al., 2023a; Maletha et al., 2020; McClelland, 2011). Ecosystems vary greatly in terms of their sensitivity to anthropogenic pressures, depending upon their nature and degree. These pressures determine the ecosystem in terms of species composition, diversity, and regeneration at the local and global scales (Bisht et al., 2022; Chaturvedi et al., 2017; Maletha et al., 2023). Antarctica's extreme geographical remoteness and environmental conditions have deterred sustained human habitation, establishing the prevailing narrative of this polar expanse as largely untouched for an extended period (Bargagli, 2008). Recent empirical observations have highlighted a disconcerting trajectory of anthropogenic contamination in Antarctica, which is intricately linked to the increasing presence of visitors and scientific undertakings (Amaro et al., 2015; Bargagli, 2008; Emnet et al., 2015; Mão de Ferro et al., 2013; Padeiro et al., 2016). This unfolding scenario underscores the importance of safeguarding Antarctic ecosystems and alleviating the repercussions of human presence in accordance with the principles articulated in the Antarctic Treaty and the Protocol on Environmental Protection to the Antarctic Treaty.

Deception Island, situated in the South Shetland Archipelago of Antarctica, stands out as a significant locale, characterized by its distinctive geological features. Specifically, the island's designation as an active volcano has resulted in the creation of a caldera-an extensive depression subsequently inundated by seawater (Baraldo and Rinaldi, 2000). The caldera, named Port Foster, exhibits a distinct horseshoe shape, opening to the Southern Ocean through a narrow channel known as Neptune's Bellows, rendering it one of the few locations globally where vessels can navigate directly into an active volcano (Baraldo and Rinaldi, 2000). Deception Island offers various tourist attractions, particularly penguins, fur seals, and whale watching (Dibbern, 2010; Naveen et al., 2012), in addition to engaging in extreme tourism (Pertierra et al., 2014).

Deception Island is one of the most naturally contaminated regions on the continent with mercury (Hg), characterized by elevated concentrations in both water and sediments (Mão de Ferro et al., 2014). At present, Deception Island hosts numerous fumaroles and hydrothermal vents located at Fumarole, Telefon, Whalers Bays, and Pendulum Cove (Rey et al., 1995), which act as the primary sources of mercury on Deception Island (Mão de Ferro et al., 2014). Additionally, the water within Port Foster exhibits a mean residence time of 2.4 years, with only 1% volume exchange occurring during each tidal cycle (Lenn et al., 2003). This limited water exchange (Figueiredo et al., 2018) results in the accumulation of particles predominantly in the western and northern regions of the bay, influenced by a gradual decrease in velocity from the Neptune Bellows to these areas. These factors, coupled with the diminished absorption of Hg in sediments driven by geological composition, contribute to the establishment of an internal reservoir of volcanic Hg accessible to aquatic organisms (Duarte et al., 2018; Mão de Ferro et al., 2014). The island also adhered to an Antarctic Specially Managed Area Management Plan under the Protocol for Environmental Protection of the Antarctic Treaty, also known as the Madrid Protocol (1991), with visitor guidelines in place to support responsible tourism. According to the International Association of Antarctica Tour Operators (IAATO), 5634 tourists visited Deception Island between 2016 and 2017 (IAATO, 2017). Hosting two summer research stations managed by Argentina (Deception station) and Spain (Gabriel de Castilla station), Deception Island witnessed the operation of Deception station for approximately 80 days with 25 individuals during the 2016-17 season, while Gabriel de Castilla station was active for 81 days, accommodating an average of 31 persons (Quesada, A., 2020, pers. comm., 17 July 2022). Both stations are equipped with waste and hazardous management facilities, and are capable of responding to fuel spills (COMNAP, 2017). The Gabriel de Castilla station has been awarded the Environmental Quality Certification ISO 14001, exemplifying efforts to diminish the environmental impact through procedural enhancements and improved waste treatment. These facts collectively underscore the human presence on this remote Antarctic Island and the ongoing commitment to minimizing environmental ramifications. Nevertheless, it is imperative to acknowledge that human activities may potentially introduce new and emerging contaminants into this locale, substances that would otherwise remain absent. Specifically for this category termed Emerging Pollutants (EPs), encompassing a wide array of synthetic chemicals such as pesticides, cosmetics, personal and household care products (PPCP), and pharmaceuticals, increasingly utilized on a global scale (Thomaidis et al., 2012). The remote and pristine environments of Antarctica are immune to the infiltration of emerging contaminants, as evidenced by studies examining the environment and wastewater from scientific stations, vessels, and cruise ships. These studies have uncovered a diverse array of contaminants, including UV filters, parabens, antimicrobial compounds, plasticizers, and pharmaceutical residues, such as estrogen steroid hormones (Duarte et al., 2021b; Emnet et al., 2015; Esteban et al., 2016). However, our understanding of the prevalence of PPCPs in the Antarctic natural environment is limited. Additionally, considering the conservation of pharmaceutical action mechanisms across a broad spectrum of organisms, understanding the potential effects of PPCPs on non-target species is of paramount significance (Duarte et al., 2021a, 2022a; Gunnarsdóttir et al., 2013). The presence of these compounds in marine areas is known to negatively affect not only primary producers (Duarte et al., 2018, 2021a) but also marine fauna that rely on them (Duarte et al., 2020; Fonseca et al., 2021) and microorganisms (Centurion et al., 2022; Duarte et al., 2022b; Zhang et al., 2022), with negative impacts on biodiversity and ecosystem functioning. While this is already a critical aspect for all ecosystems worldwide, it assumes particular concern in vulnerable ecosystems, such as polar areas, already subjected to climatic change pressures.

The inherent biogeochemical characteristics of Deception Island, coupled with escalating anthropogenic influences, render this ecosystem an optimal natural setting for investigating the impact of these pressures on the ecological and functional dynamics of marine prokaryotes and viruses, under the influence of both natural and human-induced factors. Furthermore, within the One-Health Framework (Ewbank et al., 2021), the identification and evolution of prokaryotic resistance genes are critical, offering insights into how these conditions mold the marine polar resistome, inducing the appearance of Antibiotic and Metal Resistance Genes (ARGs and MRGs, respectively) in the prokaryotic community. A recent work focusing on a terrestrial volcanic system, highlighted the co-influence of the heavy metals released by volcanic systems, with the inherent abiotic factors in the vicity of an active volcano (for e.g., pH) in shapping the sensitivity/resistance of the microorganisms towards heavy metals, reinforcing the need to better understand these associations in the development of MRGs (Chen et al., 2024). Several studies have explored prokaryotic metagenomic diversity within Antarctica, with a specific focus on Deception Island (Centurion et al., 2022; Santos et al., 2022), particularly emphasizing function and resistance traits, predominantly in the island's soils. The unique environmental conditions of Deception Island are significant because of documented instances of co-resistance phenomena involving metals, harsh environmental conditions, and antibiotics in environments that are minimally influenced by human activity (Duarte et al., 2022b; Jardine et al., 2019). Therefore, it is essential to monitor these microorganisms, not only because of their fast response time, which allows them to act as early warning sentinels, but also because of their key role in the ecosystem's biogeochemical functioning (which impacts all organisms that inhabit the ecosystem) and the potential emergence of multi-resistant microorganisms that can ultimately impact human health.

Considering the two major ecosystem pressure sources in Deception Island's inner bay marine waters (volcanic and anthropogenic), it is hypothesized that these would lead to differential impacts on the prokaryotic and viral community taxonomic and functional traits, leading to the potential existence of singular features that could discriminate

Fig. 1. Sampling sites were located in the vicinity of the Spanish Gabriel de Castilla Base (GdC) and at Fumarole Bay (FB), both situated in Foster Bay, Deception Island, South Shetland Islands archipelago, Antarctica.

Table 1
Surface water physical and chemical characteristics, namely pH, conductivity, dissolved oxygen (DO), salinity and suspended particulated matter (SPM) in the two sampling sites, Gabriel de Castilla and Fumarole Bay (average ± standard error, N = 3, * denotes statistical differences at $p < 0.05$) (Duarte et al., 2018).

	Temperature (°C)	pH	Conductivity (μS cm^{-1})	DO (%)	Salinity	SPM (mg L^{-1})
Gabriel de Castilla	3.5	8.35	59.7	124.9	38.3	23.8 ± 0.6
Fumarole Bay	3.8	8.12	63.7	127.5	41.0	38.2 ± 1.0 *

between these two main sources of impacts. Hence, the present study aimed to elucidate the ecological, functional, and resistome traits of prokaryotic and viral marine communities in the waters surrounding Deception Island. Special attention was given to two distinct sampling sites, namely, Fumarole Bay and waters in the vicinity of Gabriel de Castilla station, each influenced by different volcanic and anthropogenic factors. Additionally, this study sought to unveil potential taxonomic and functional indicators (biomarkers) associated with these diverse pressures. These indicators may serve as valuable tools for future assessments of potential shifts in marine ecosystem dynamics on the island influenced by both natural and anthropogenic sources.

2. Material and methods

2.1. Study area characterization and sample collection

Sampling was conducted in Port Foster Bay, situated within Deception Island (62°57′S, 60°38′W) in the South Shetland Islands of Antarctica, during the austral summer of January 2017. Sampling was conducted in the proximity of the Spanish Gabriel de Castilla station and Fumarole Bay (Fig. 1). Surface water samples were collected and transported under refrigeration using ice blocks to the laboratory at the Gabriel de Castilla Spanish station. All samples were processed in the laboratory, as previously described (Duarte et al., 2022b). The samples were filtered using 0.22 μm pore size Sterivex filters (Merck Millipore) without pre-filtration and were kept at −80 °C before transportation to Portugal in liquid nitrogen. In situ measurements of water physico-chemical parameters, including temperature, pH, conductivity, dissolved oxygen (DO), and salinity, were conducted using a multiparameter probe (WTW, Multi 3430). Surface water was collected in triplicate to determine suspended particulate matter (SPM). The probe measurements represent the outcome of three readings automatically performed by the probe. Despite the unique characteristics of Deception Island (an open ocean bay resulting from a caldera collapse with active submarine volcanic activity), its marine environment shares common features with other marine systems (Table 1) (Duarte et al., 2018).

2.2. DNA extraction and metagenomic sequencing

At the BioISIGenomics facilities, the Sterivex filters were opened and removed using a sterile scalpel and tweezers, as demonstrated in the video: https://vimeo.com/26582858. Subsequently, the filters were placed into a 5 mL PowerWater Bead Pro Tube from the DNeasy PowerWater Kit (Qiagen), using two sets of sterile forceps. This was achieved by picking up the filter membrane at opposite edges and rolling the filter into a cylinder, with the top side facing inward. The remaining steps were performed in accordance with the manufacturer's instructions. DNA quality and concentration were assessed by NanoDropTM One and QubitTM 4 Fluorometer analyses using the dsDNA HS assay for Qubit. Three biological replicates were obtained for each sampling point and used as independent samples. Quantification was performed using the dsDNA HS assay for Qubit. DNA was end-repaired (New England BioLabs, MA, USA), cleaned with Agencourt AMPure XP Beads (Beckman Coulter, High Wycombe, UK), and dA-tailed (New England BioLabs, MA, USA). The library was prepared from 1400 ng of input DNA using the SQK-LSK109 kit (Oxford Nanopore Technologies, Oxford, UK), following the manufacturer's protocol. The library was quantified and prepared for GridION sequencing using FLO-MIN106 flow cells, MinKNOW v18.12.4, standard 48-h run script with active channel selection enabled, until 4.0 Gb of data was collected from each sample. The mean read length of the sequenced reads was 2900 bps and the mean quality score was 9.85.

2.3. Bioinformatic analysis

The site-associated metagenome was identified by long-read whole-genome sequencing of the environmental samples. A total of 2.22 million reads were acquired, and reads with a length of ≥300 base pairs, accompanied by quality scores ≥7, were selected for subsequent taxonomic analysis. For taxonomic reconstruction, 1.69 million reads were employed, and a custom in-house pipeline relying on k-mer taxonomic classification identified 1.11 million reads. The analytical pipeline starts with Prinseq-lite version 0.20.4 (Schmieder and Edwards, 2011) to remove the reads with less than 300 bps and with a dust score, for reduction of read complexity, below 7. Taxonomic classification was performed using Kraken2 (version 2.1.2), running on default options

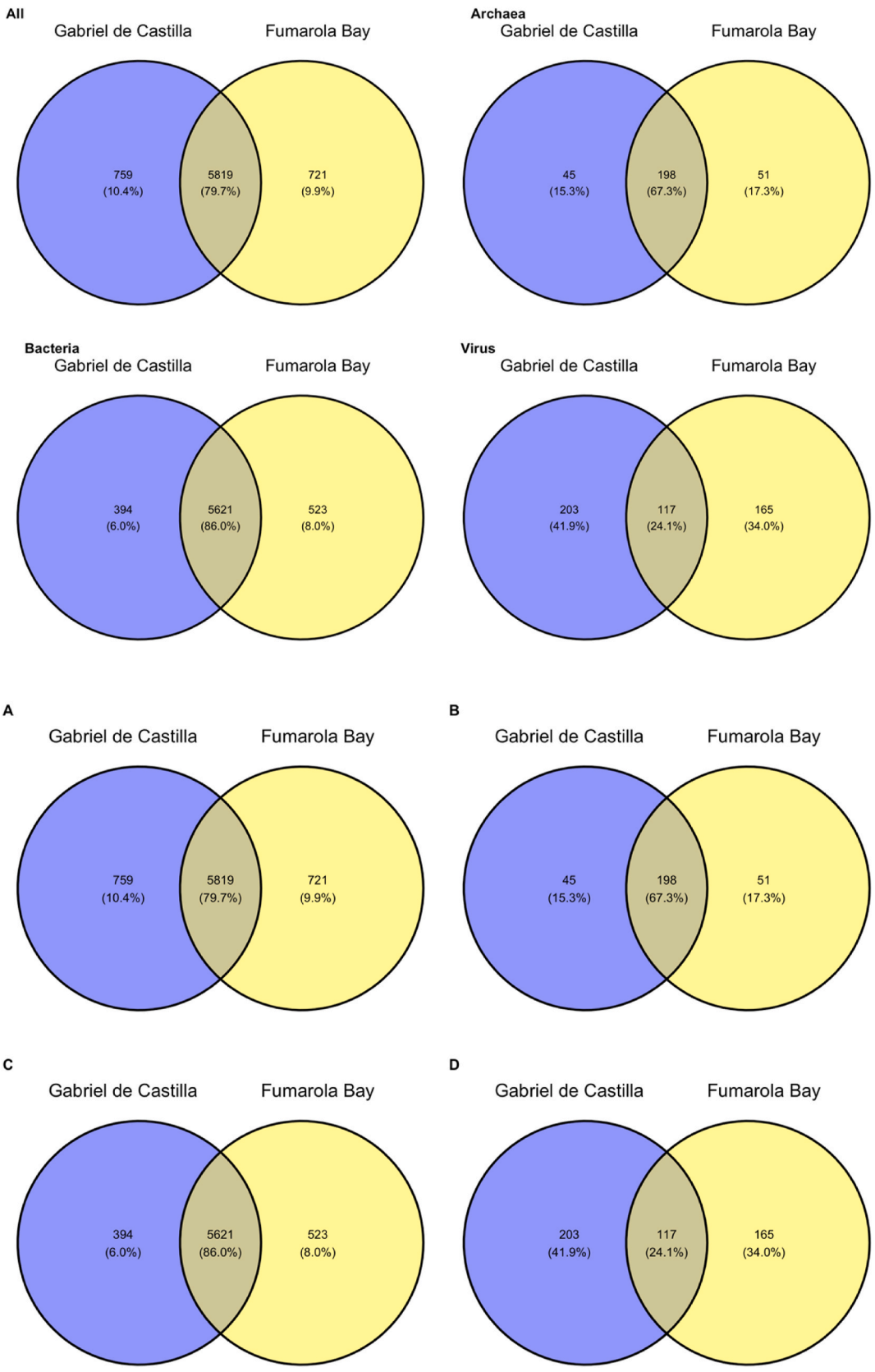

Fig. 2. Venn diagrams showing all OTUs from the three analyzed kingdoms (A) and for each kingdom individually (B, Archaea; C, Bacteria; D, Virus) detected in the water samples collected at Fumarole Bay and Gabriel de Castilla sampling sites.

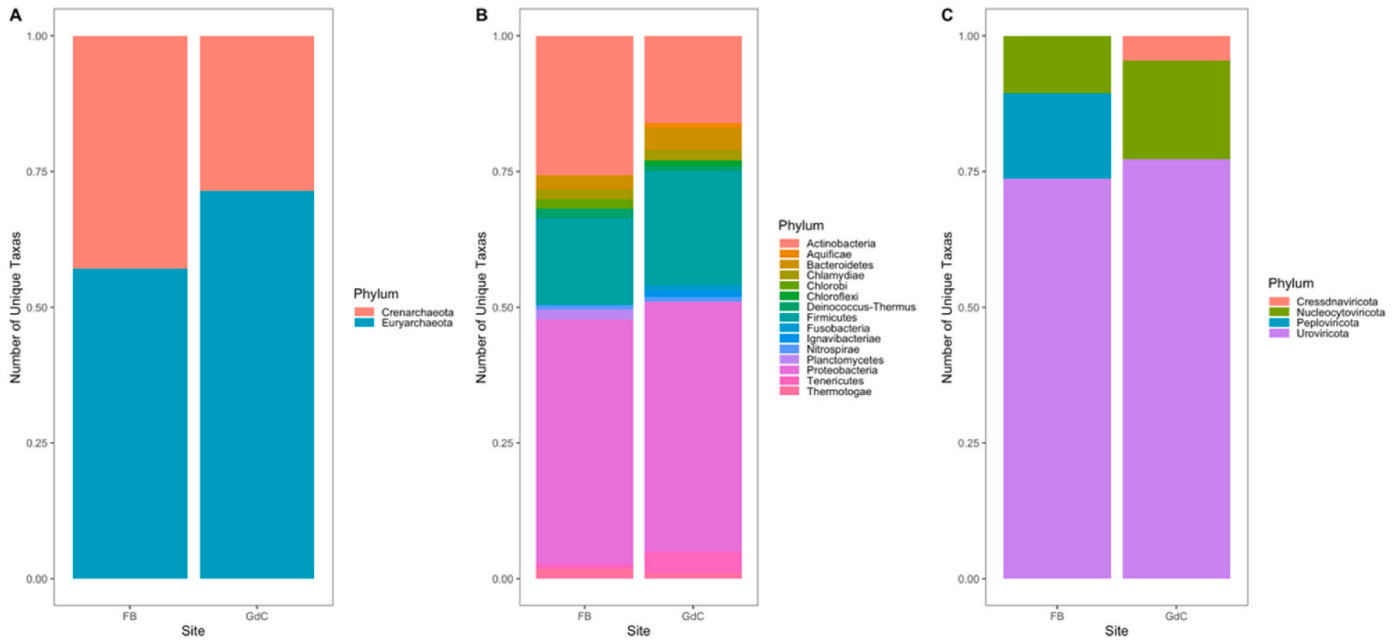

Fig. 3. The number of unique Archaea (A), Bacteria (B), and Virus (C) phyla (normalized to the total number of unique phyla per kingdom) detected in the water samples collected at Fumarole Bay (FB) and Gabriel de Castilla (GdC) sampling sites.

and with the NCBI Refseq database (Archaea, Bacteria, and Viruses) to merge assignments into the highest common taxonomic rank (LCA) (Wood et al., 2019).

Only Operational Taxonomic Units (OTUs) with a prevalence in all three replicates obtained from each sampling site were retained for analysis (a total of 9976 OTUs). Rarefaction, alpha, and beta diversity analyses were conducted using the *phyloseq* package (McMurdie and Holmes, 2013) in R-Studio Version 1.4.1717. The statistical significance of the diversity metrics and abundance data between sampling sites was assessed by Student's t-test using the *ggpubr* package (Kassambara, 2023) in R-Studio Version 1.4.1717.

Heat trees were produced using the *metacoder* package (Foster et al., 2017) in R-Studio Version 1.4.1717. Only OTUs with a complete taxonomic lineage were used to avoid a taxonomic bias at the upper taxonomic levels. Standard data preprocessing was performed according to the manufacturer's instructions. Briefly, zero- and low-abundance OTUs were removed (counts <5), and data were normalized for uneven sampling (Foster et al., 2017). The Davidson-Harel visualization layout was used, and the Reingold-Tilford algorithm was used for node locations. Significant differences in the abundance of specific taxonomic levels in both sample groups were evaluated using the built-in Wilcoxon test of the *metacoder* package. Sample dissimilarity dendrograms were generated using the *phyloseq* package (McMurdie and Holmes, 2013) in R-Studio Version 1.4.1717 using Jaccard distance as a dissimilarity measure.

Functional analysis of the prokaryotic community was performed with the *microeco* R package using the prokaryotes database FAPROTAX (Liu et al., 2021; Louca et al., 2016) in R-Studio Version 1.4.1717.

For resistome analysis, Diamond blastx (v2.1.8.162) was used to align the reads against the NCBI nr database (July 2023). To obtain the metal-resistance genes (MRGs), reads were aligned against the BacMet database (Pal et al., 2014) using blastx (v2.14.0+) with the following parameters: E-value cutoff = 1×10^{-20}; Number of aligned sequences to keep = 5; Percent query coverage per hsp (%) = 80. The presence of Antibiotic Resistance Genes (ARGs) was assessed using the ARGs Desktop software ("ARGs Desktop: A cross-platform desktop software for antibiotic resistance genes detection and analysis from metagenomic data," 2023) using an E-value cutoff = 1×10^{-20}, E-value cutoff for Essential Single Copy Marker Genes of 3 and Identity cutoff (in percentage) for Essential Single Copy Marker Genes of 45%. Annotation of the detected ARGs into antibiotic resistance classes was performed using the ResistoXplorer web-based database (Dhariwal et al., 2021).

Partial Least-Squares Discriminant Analysis (PLS-DA) was performed using the *DiscriMiner* package (Sanchez, 2013) in R-Studio Version 1.4.1717. The number of components was set to 2. Variable importance for model classification was evaluated using the Variable Importance in Projection (VIP) parameter.

For the identification of potential site-associated indicator OTUs and functional and resistome traits, two approaches were used: correlation index analysis based on the point biserial correlation coefficient and Variable Importance for Projection Partial Least-Squares Discriminant Analysis (VIP-PLS-DA). OTUs, functional and resistome traits were identified as potential site-associated indicator species or traits when three criteria were met: biserial correlation coefficient >0.90, P-value from the correlation index analysis was <0.05, VIP score >1. Correlation indices analysis, indicating OTUs, functional or resistome traits that are significantly ($p < 0.05$) associated with a given sampling site, was performed using the R package *indicspecies* (Cáceres and Legendre, 2009) in R-Studio Version 1.4.1717.

3. Results

3.1. Prokaryotic and viral taxonomic diversity and composition

Following the application of rarefaction (Fig. S1), an enumeration of 9976 distinct microbial taxa was achieved, with 7140 taxa classified at the species level. These taxa were further categorized into Bacteria (8749 Operational Taxonomic Units - OTUs), Viruses (703 OTUs), and Archaea (522 OTUs). Collectively, both the prokaryome and virome exhibited taxonomic diversity encompassing 62 phyla, 119 classes, 248 orders, 549 families, and 2110 genera.

Considering all OTUs identified within the Archaea, Bacteria, and Virus kingdoms, approximately 80% of these OTUs were shared across both sampling sites (Fig. 2). Nonetheless, it is noteworthy that each site exhibited more than 700 exclusive OTUs. A consistent pattern emerged in the taxonomic groups Archaea, Bacteria, and Virus kingdoms. Specifically, archaeal OTUs presented the lowest number of exclusive occurrences at each site, between 45 and 51. Conversely, the Bacteria

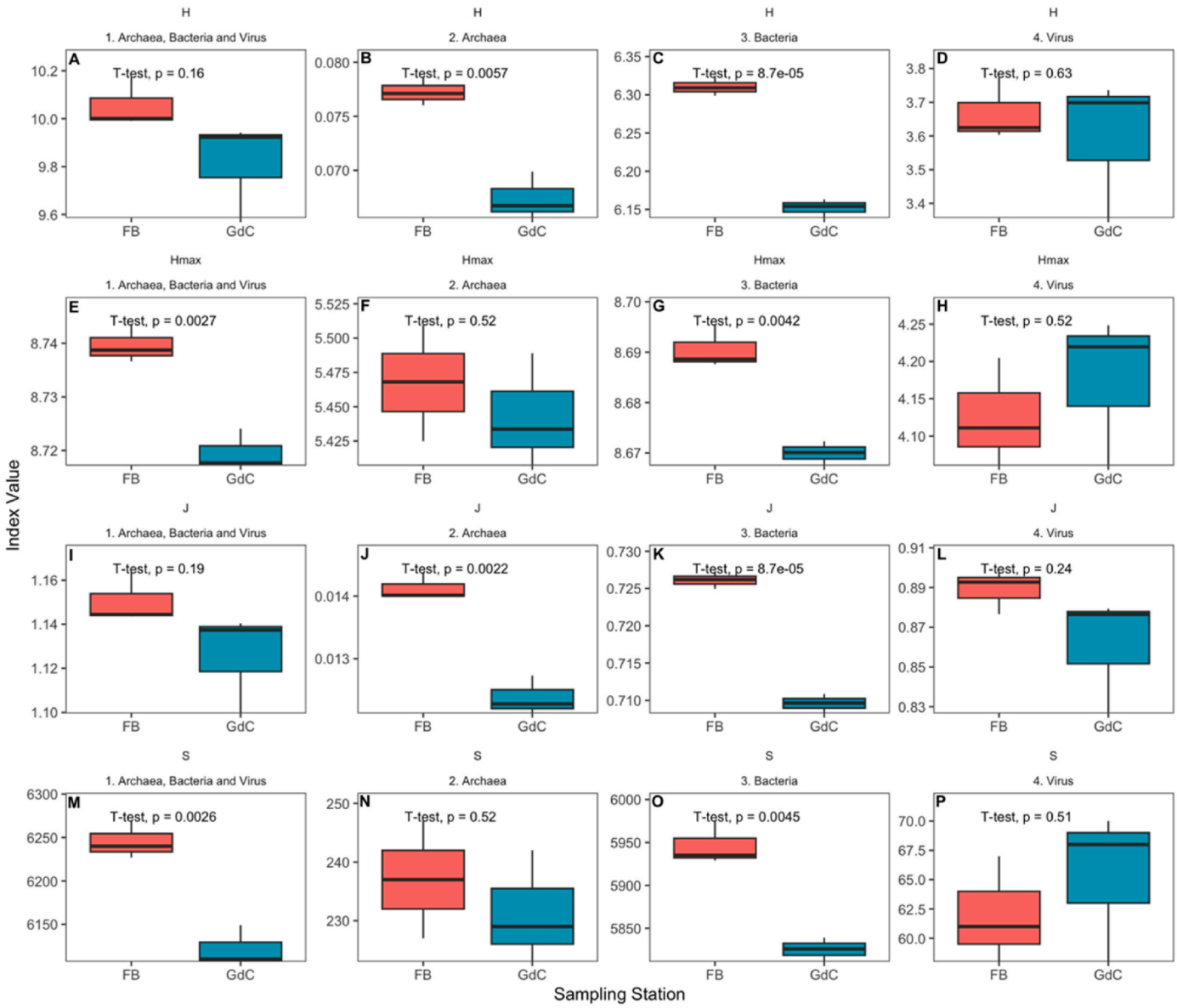

Fig. 4. Diversity indices, namely Shannon Diversity (H, panels A–D) and Maximum Diversity (Hmax, panels E–H), Pielou Equitability (J, panels I–L) and Specific Richness (S, panels M–P) of the three considered Kingdoms combined (A, E, I and M) or for each kingdom OTUs (Archaea: panels H, F, J and N; Bacteria: panels C, G, K and O; Virus: D, H, L and P) detected in the water samples collected at Fumarole Bay (FB) and Gabriel de Castilla (GdC) sampling sites (N = 3; T-test indicates the Student's t-test statistical significance value).

kingdom showed the highest number of OTUs shared between both sampling sites (a total o 5621 shared OTUs representing 86 % of the Bacteria OTUs). Notably, the Fumarole Bay samples exhibited a greater number (523) of OTUs exclusive to that sampling station. In contrast, Virus OTUs demonstrated a smaller shared proportion between the two sites (24%), with a significant number of OTUs exclusively found in samples collected at Gabriel de Castilla station (203 OTUs, 41.8%) and Fumarole Bay (166 OTUs, 34.2%).

Upon further examination of the distinct OTUs present in the microbial communities within Deception Island, notable variations in the community composition were observed (Fig. 3). A focused scrutiny of the Archaea community disclosed that Fumarole Bay exhibited a heightened number of unique Crenarchaeota OTUs (42.9%) when compared to the samples obtained near the Gabriel de Castilla station. Conversely, in the latter, the prevalence of exclusive Euryarchaeota OTUs was more conspicuous, constituting 71.4% of the unique Archaea phylum OTUs (Fig. 3A). In the realm of unique bacterial OTUs (Fig. 3B), discernible differences were observed, particularly with Actinobacteria, where Fumarole Bay manifested approximately 25.7% of all unique OTUs belonging to this phylum, in contrast to only 16.0% in samples from Gabriel de Castilla base. Furthermore, the Fumarole Bay samples revealed the presence of four exclusive Chlorobi and Planctomycetes OTUs (two from each phylum), whereas these phyla lacked any exclusive OTUs in samples near the Gabriel de Castilla base. Conversely, the latter samples contained unique OTUs from Aquificae, Chloroflexi, Fusobacteria, and Ignavibacteriae, which were not found among the unique phyla detected in Fumarole Bay, each displaying a singular OTU. Interestingly, both sampling sites exhibited a similar proportion of unique OTUs within Firmicutes (16.0% and 21.0% at Fumarole Bay and GdC base, respectively) and Proteobacteria (45.1% and 46.0% at Fumarole Bay and GdC base, respectively), which were two of the most abundant phyla in the samples. In terms of unique viral OTUs, Fumarole Bay presented three exclusive Peploviricota OTUs, a phylum without any unique OTUs, in samples near the Gabriel de Castilla base (Fig. 3C). Conversely, the samples from the vicinity of the Spanish base revealed one unique OTU belonging to the phylum Cressdnaviricota, which

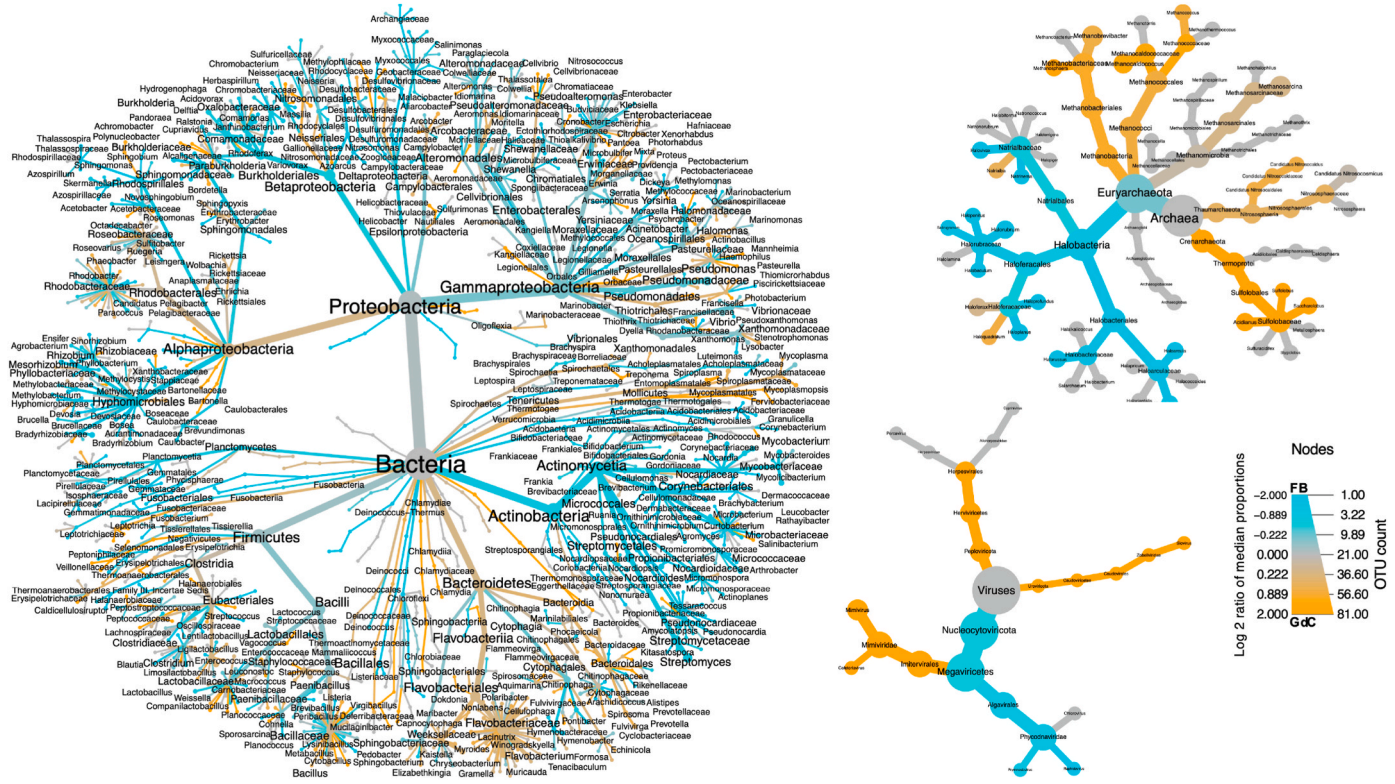

Fig. 5. Archaea, Bacteria and Virus comparative heat trees showed significantly different taxonomic node abundances in the water samples collected at Fumarole Bay (FB, blue branches) and Gabriel de Castilla (GdC, orange branches) sampling sites (N = 3). Heat trees represent a visualization of community data within a taxonomic framework by associating any statistical metric with the color or size of the tree components. The color scheme denotes the abundance of OTUs significantly more prevalent at either Fumarole Bay station (depicted in blue) or Gabriel de Castilla station (depicted in orange). The width of the nodes represents the OTU counts attributed to each taxon, whereas the thickness of the edges represents the number of associated reads. For clarity, taxa with ambiguous names and those that were absent in more than 30% of the samples were excluded from the visualization. (For interpretation of the references to color in this figure legend, the reader is referred to the Web version of this article.)

lacked any unique OTUs in Fumarole Bay. Approximately 73.7% and 77.3% of the total unique viral OTUs in Fumarole Bay and in the vicinity of the Spanish base, respectively, belonged to the phylum Uroviricota. Two unique viral OTUs (10.5% of the total unique viral OTUs) in Fumarole Bay pertain to Nucleocytoviricota, whereas 18.2% of the total unique viral OTUs from this phylum were detected near the Gabriel de Castilla base.

Considering the diversity of the samples obtained from both sampling sites (Shannon Diversity index, H), discernible patterns emerged, wherein no significant differences were evident when considering all surveyed kingdoms or the virus kingdom alone (Fig. 4A). However, notable disparities in Archaea and Bacteria diversities were evident (Fig. 4B and C), with samples from Fumarole Bay exhibiting significantly higher diversities. A more in-depth analysis of the maximum Shannon diversity index (Hmax), encompassing all evaluated kingdoms (Fig. 4E) or the Bacteria kingdom exclusively (Fig. 4G), revealed a markedly higher index in the metagenomes collected at Fumarole Bay. In terms of evenness, only Archaea OTUs exhibited a higher Pielou index value in Fumarole Bay (Fig. 4J) in contrast to the values observed for samples from the Gabriel de Castilla sampling station. Furthermore, the Bacteria kingdom displayed significantly higher specific richness (S) in metagenome samples from Fumarole Bay (Fig. 4O). This augmented value contributed to an overall higher S value for all kingdoms, culminating in a global S value that was significantly higher than that observed in the Gabriel de Castilla samples (Fig. 4M). It is essential to highlight that the reduced number of Archaea species (Fig. 4N) and their relative abundance resulted in a considerably lower value for the Shannon diversity index within this kingdom (Fig. 4B), juxtaposed with the values obtained for the remaining kingdoms.

The utility of the heat trees is underscored in Fig. 5, revealing numerous clades in the tree that are exclusive to samples from one of the surveyed sites, often encapsulating the entire taxonomic group. Notably, the clades predominantly featured Alphaproteobacteria and Bacteroidetes in Gabriel de Castilla station samples and Gammaproteobacteria and Actinobacteria in the Fumarole Bay metagenomes. Additionally, at lower taxonomic lineage levels (genus and node outer edges), the heat trees accentuated the pronounced differences in taxonomic composition between the two sampling stations, reflecting the high abundance of several significant disparities. Despite the relatively less complex nature of the Archaea heat tree, evident distinctions emerged, including a noteworthy prevalence of Halobacteria OTUs (and their lower taxonomic lineage levels) in Fumarole Bay metagenomes, whereas Gabriel de Castilla samples exhibited a prevalence of other Archaea groups, such as Methanobacteria, Methanococci, and Crenarchaeota. In the context of the viral tree, it exhibited significantly lower complexity than Bacteria and Archaea. Fumarole Bay displayed a marked prevalence of Algavirales in contrast to Gabriel de Castilla metagenomes, which were prominently dominated by Imitervirales, Paploviricota, and Uroviricota (and their respective lower taxonomic branches).

Employing a dissimilarity analysis based on the Jaccard distance within and between samples collected at each site (Fig. 6), we assessed the contribution of each kingdom's taxonomic composition to the dissimilarity observed between the samples from both sites. Despite certain differences in alpha diversity indices between sites, an examination of the Archaea phyla revealed that the Jaccard dissimilarity distance between sites closely mirrors the dissimilarity observed within site replicates. This suggests a high degree of similarity in the relative abundance of Archaea phyla between the two sampling sites (Fig. 6A).

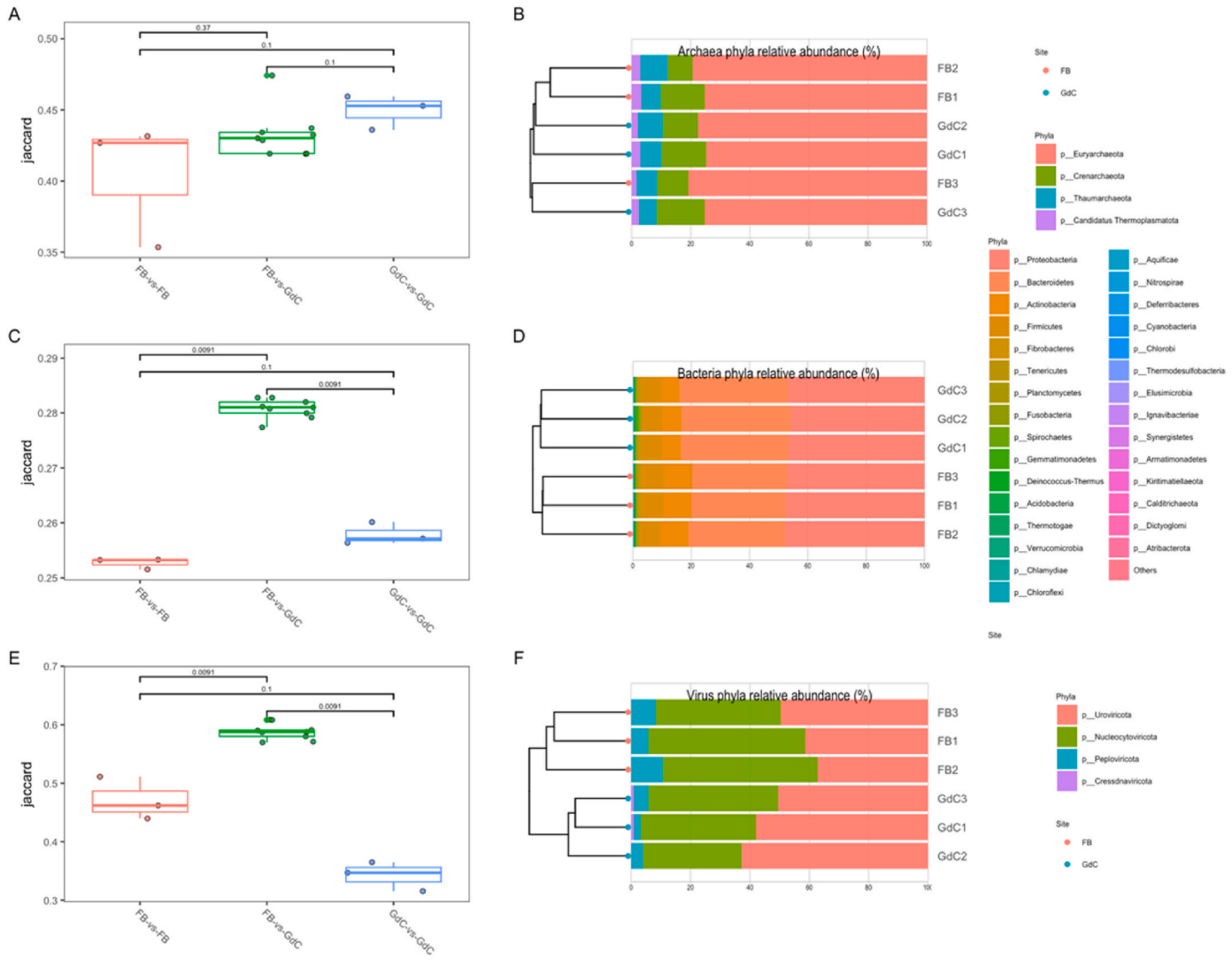

Fig. 6. Archaea, Bacteria and Virus phyla-based Jaccard distance between sample groups (A, C and E respectively) and respective relative rarefied abundance dendrogram (normalized for the total abundance in each Kingdom; B, D and F for Archaea, Bacteria and Virus respectively) in the water samples collected at Fumarole Bay (FB) and Gabriel de Castilla (GdC) sampling sites (N = 3; significant level between Jaccard distances between sample groups are denoted as Student's t-test p-value).

Consequently, a lack of separation was evident in the respective abundance dendrogram (Fig. 6B), where all samples were predominantly characterized by Euryarchaeota, Crenarchaeota, and Thaumarchaeota. In the context of dissimilarity distances among replicate samples and between samples from different sampling sites concerning the relative abundance of bacterial and viral phyla (Fig. 6C and E), in both instances, the dissimilarity between sampling sites surpassed the observed dissimilarity within replicate samples. This distinction was further evidenced in the corresponding dendrograms built using bacterial (Fig. 6D) and viral (Fig. 6F) phyla relative abundance, where samples from both sites were distinctly separated. Bacterial abundance was primarily dominated by the Proteobacteria, Bacteroidetes, and Actinobacteria phyla, collectively constituting approximately 90% of the relative abundance of OTUs within the bacterial kingdom. Regarding the relative abundance of viral phyla, OTUs were predominantly affiliated with Uroviricota and Nucleocytoviricota, displaying varying relative proportions in samples collected from both sampling sites.

Analyzing the relative abundance of phyla exhibiting marked differences between sampling stations, an evident predominance of Archaea was shown by the prevalent OTUs from the Fumarole Bay metagenomes (Fig. 7A), particularly of the phylum Euryarchaeota (Fig. 7B). Conversely, within the Bacteria kingdom, a significant prevalence was discerned in metagenome samples from Gabriel de Castilla (GdC) (Fig. 7C), primarily attributable to the significantly higher abundance of Bacteroidetes (Fig. 7E), Balneolaeota (Fig. 7F), Fusobacteria (Fig. 7I), Ignavibacteriae (Fig. 7J), and Tenericutes (Fig. 7M), in contrast to the relative abundance observed in Fumarole Bay (FB) samples. The latter group exhibited a marked prevalence of Actinobacteria (Fig. 7D), Chrysiogenetes (Fig. 7G), Planctomycetes (Fig. 7K), Synergistetes (Fig. 7L), and unassigned bacterial phyla (Fig. 7N). Notably, the only viral phylum displaying significant abundance differences at both survey sites was Nucleocytoviricota (Fig. 7O), with higher levels observed in the Fumarole Bay samples.

3.2. *Bacteria and Archaea: functional diversities*

Several distinctions emerged regarding the putative metabolic functional profiles observed in the samples collected at both surveyed sites (Fig. 8). The traits attained from this functional analysis should be considered putative or potential functions and should be interpreted as measured microbial activities. Chemoheterotrophic functions were notably more abundant in the Gabriel de Castilla samples (Fig. 8A and

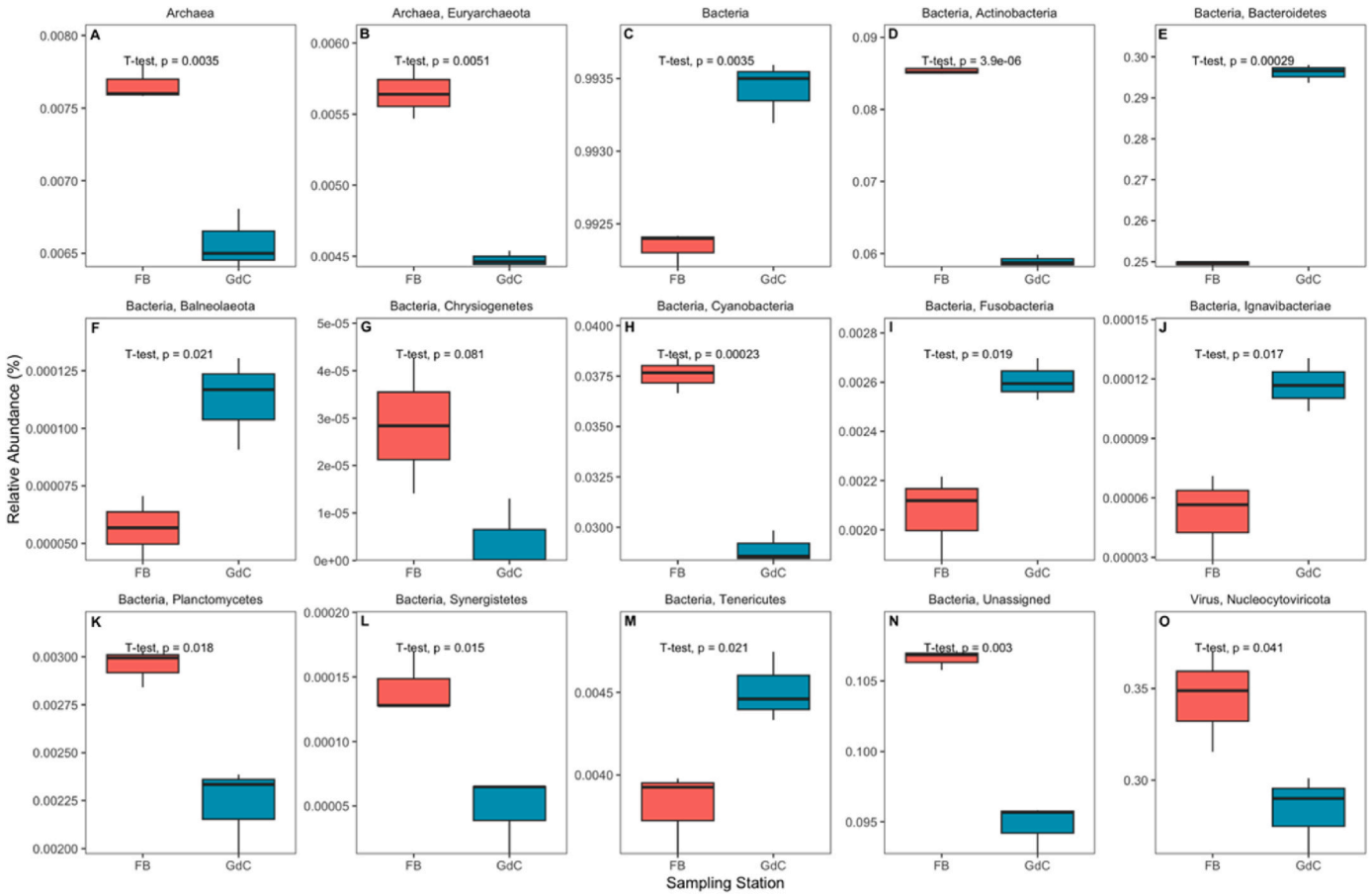

Fig. 7. Relative abundance (normalized for the total abundance considering all hits from all Kingdoms) of the significantly different Archea (A–B), Bacteria (C–N) and Virus (O) OTU taxonomic phyla detected in the water samples collected at Fumarole Bay (FB) and Gabriel de Castilla (GdC) sampling sites (N = 3; T-test indicates the Student's t-test statistical significance value).

F). Conversely, the Fumarole Bay samples exhibited a significantly higher abundance of microorganisms with the potential ability to degrade aromatic and hydrocarbon compounds (Fig. 8B–D and M). Putative metal-based metabolic activities were also more prevalent in the metagenome samples from Fumarole Bay (Fig. 8E–H, I, and P). Microbial nitrogen, sulfur, and phototrophic metabolism displayed a similar pattern, with all functions associated with these metabolic pathways being more abundant in the Fumarole Bay samples (Fig. 8G–R-V, X, and Y). Samples collected in the vicinity of Gabriel de Castilla station showed a prevalence of microorganisms with the potential to act as human pathogens associated with gastrointestinal conditions (Fig. 8J), while microbes with the potential to lead to nosocomial and pneumonia pathogenic conditions were significantly more abundant in Fumarole Bay samples (Fig. 8K and L). Potential activities related to the degradation of plastic (Fig. 8W), lignomaterials (Fig. 8N), and urea (Fig. 8Z) were significantly more abundant in the Fumarole Bay samples. Additionally, the potential methanogenic metabolism associated with CO_2 reduction using H_2 was notably more abundant in samples collected near Gabriel de Castilla station (Fig. 8O).

Analysis of the presence of metal resistance genes (MRGs) and antibiotic resistance genes (ARGs) in samples obtained from Fumarole Bay and Gabriel de Castilla sampling stations revealed discernible differences (Fig. 9). While overall ARGs and MRGs displayed significant differences between the sampling sites, a deeper analysis of the individual MRG groups revealed additional distinctions. Silver (Ag), iron (Fe), magnesium (Mg), and vanadium (V) resistance genes were notably more abundant in the samples collected from Fumarole Bay. Conversely, gold (Au) and antimony (Sb) resistance genes were significantly more abundant in samples collected at the Gabriel de Castilla site. Similarly, analysis of specific antibiotic-type resistance genes revealed disparities between samples from both sites. Macrolide, bacteriostatic, aminocoumarin, multidrug, pleuromutilin, and mupirocin-like resistance genes were significantly more abundant in the samples collected at the Gabriel de Castilla site. Conversely, genes associated with resistance to tetracycline, aminoglycoside, peptide, nitroimidazole, diaminopyridine, and lincosamide-type antibiotics displayed an inverse trend, with a significantly higher abundance in samples collected from Fumarole Bay. A total of 13 ARG types were identified in samples from the vicinity of the Gabriel de Castilla base, compared with 11 ARG traits detected in samples from Fumarole Bay. Notably, genes related to bacteriostatic, pleuromutilin, oxazolidinone, and mupirocin-like antibiotic resistance were absent in the Fumarole Bay samples, whereas genes associated with resistance to diaminopyrimidine and lincosamide were exclusively found in samples from this sampling site.

3.3. *Taxonomic and functional indicators*

The taxonomic, functional, and resistome profiles of samples collected near Gabriel de Castilla station and at Fumarole Bay have proven to be highly effective discriminators of both prokaryotic and viral communities, resulting in a distinct separation evident in the Partial Least Squares Discriminant Analysis (PLS-DA) biplots (Fig. 10A, B, and 10C). Considering the contribution of OTUs, functional traits, and resistome features for each statistical model, it was determined that approximately 2526 OTUs, 43 functional traits, and 18 resistome features (Fig. 10D, E, and 10F), collectively accounting for 38.0%, 48.3%, and 51.4% of the Variable Importance in Projection (VIP) scores, respectively, exhibited VIP scores above 1, indicating a substantial

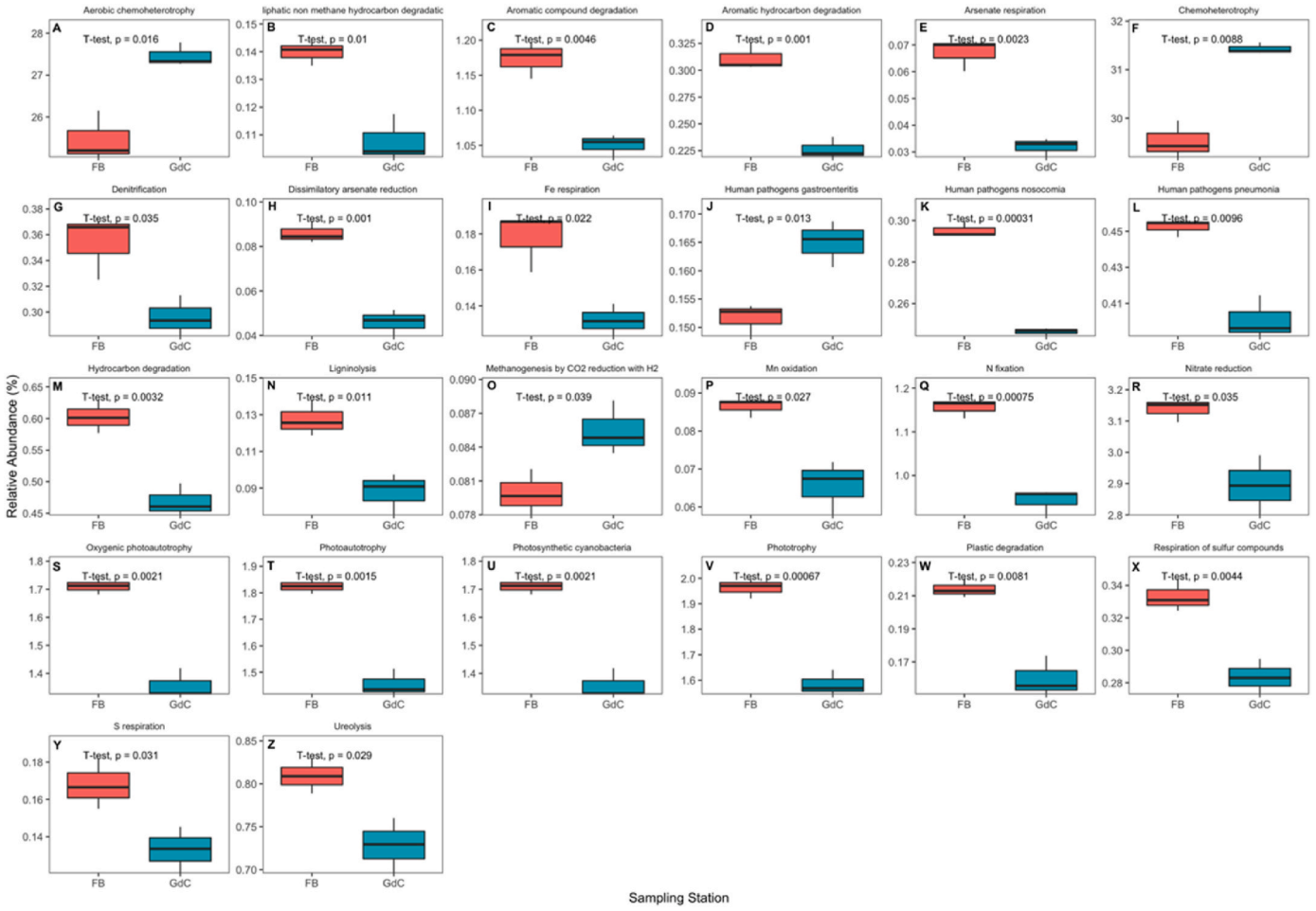

Fig. 8. Relative abundance of the significantly different putative prokaryotic metabolic functional groups detected in the water samples collected at Fumarole Bay (FB) and Gabriel de Castilla (GdC) sampling sites (N = 3).

contribution to the effective separation observed in the models.

Integrating the VIP score information with insights derived from indicator species, functional, and resistome analyses allowed for the identification of potential biomarker OTUs and functional traits using point biserial analysis (threshold set at > 0.90). This analysis was cross-referenced with OTUs, functional traits, and resistome features with a VIP score above 1 (Fig. 11A, B, and 11C). Employing this approach facilitated the depiction of site-specific biomarkers at both taxonomic and metabolic levels within the sampled metagenomes. Indicator species analysis revealed the existence of 831 and 851 OTUs with potential indicator values in the samples collected at Gabriel de Castilla and Fumarole Bay, respectively (Supplementary Fig. S2). The analysis highlighted the dominance of Euryarchaeota within the Archaea Kingdom at both sites, resulting in nine different Euryarchaeota OTUs being extracted as indicator species for each sampling site (Supplementary Figs. S2A and B). Regarding the Bacteria Kingdom (Supplementary Figs. S2C and D) the indicator OTUs extracted were dominated by Proteobacteria (394 and 330 for Gabriel de Castilla and Fumarole Bay samples, respectively), Actinobacteria (245 and 235 for Gabriel de Castilla and Fumarole Bay samples, respectively) and Firmicutes (76 and 120 for Gabriel de Castilla and Fumarole Bay samples respectively) (Supplementary Figs. S2C and D). The fourth phylum with the highest number of OTUs with indicator values was found to be different between sampling sites, with Cyanobacteria occupying the fourth group with a higher number of indicator OTUs in the samples collected at Fumarole Bay, whereas Actinobacteria occupied the fourth position in the ranking of the phylum with more indicator OTUs in the samples collected in the vicinity of Gabriel de Castilla. Only two viral OTUs were selected as indicator OTUs for the samples collected at Fumarole Bay, one belonging to the Nucleocytoviricota and another OTU to which it was not possible to assign a phylum from the sequences retrieved) (Supplementary Figs. S2E and F). On the other hand, the indicator species analysis of the data from the samples collected in the vicinity of Gabriel de Castilla resulted in the identification of 16 viral OTUs with potential indicator values (9 belonging to the Uriviricota phylum, 2 from the Nucleocytoviricota phylum and five additional OTUs to which it was not possible to assign a phylum). These indicator OTUs were further filtered by combining indicator species point-biserial statistics with their VIP scores. Based on statistical criteria, 238 OTUs were identified as eligible site-specific biomarkers (Fig. 11A). Approximately 42.9% of these OTUs were identified as specific biomarkers for the Fumarole Bay metagenomes, while the remainder were exclusive indicators of metagenomes from the vicinity of the Gabriel de Castilla station. Archaea OTUs constituted 31.9% of the assessed indicator OTUs, with 13.4% and 18.5% associated with Fumarole Bay and Gabriel de Castilla stations, respectively, all belonging to the Sulfolobaceae family. Virus OTUs accounted for 10.5% and 15.1% of the indicator OTUs in samples from Fumarole Bay and Gabriel de Castilla station, respectively (25.6% of all assessed OTUs), and all belonged to the Siphoviridae family. Bacterial OTUs from the Planctomycetaceae, Anaplasmataceae, Rickettsiaceae, and Thermodesulfobacteriaceae families constituted 18.9% and 23.5% of the indicator OTUs for the Fumarole Bay and Gabriel de Castilla stations, respectively. Despite overlap at the family level, these OTUs represented different taxonomic units,

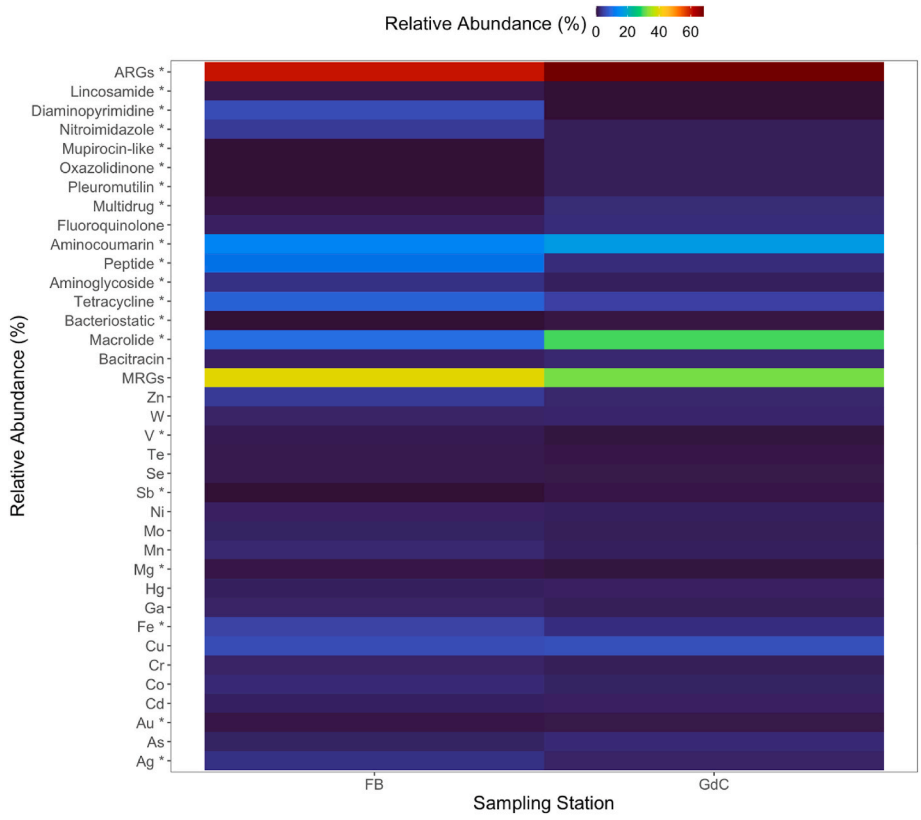

Fig. 9. Antibiotic and Metal Resistance Genes (ARGs and MRGs, respectively) relative abundance (normalized for the total number of resistance gene hits) heatmap of the water sample prokaryome collected at Fumarole Bay (FB) and Gabriel de Castilla (GdC) sampling sites (N = 3; asterisks denote the Student's t-test statistical significance differences between the abundance of a resistance gene at both sampling stations at $p < 0.05$).

demonstrating the discriminatory power between the two sites. Notable differences were evident in the context of functional traits with potential biomarker utility (Fig. 11B). Following statistical filtration, only three metabolic traits were deemed site-specific for the metagenomes near the Gabriel de Castilla station (human pathogens gastroenteritis, chemoheterotrophy, and aerobic chemoheterotrophy), while the remaining 20 traits exhibited biomarker discriminatory power for Fumarole Bay metagenomes. A similar analysis of resistome traits, identified as crucial for sample differentiation through VIP and biserial correlation, revealed six distinct resistome trait indicators for each community at the sampling sites (Fig. 11C). Tetracycline-, peptide-, nitroimidazole-, magnesium-, diaminopyrimidine-, and Ag resistance-related genes were identified as site-specific indicators for the prokaryotic community collected in Fumarole Bay. Conversely, genes associated with resistance to Sb, pleuromutilin, oxazolidinone, mupirocin-like, macrolide, and aminocumarins were identified as statistically relevant resistome indicators for the prokaryotic community near the Gabriel de Castilla station.

When summing the relative abundance (calculated for each dataset) of the traits highlighted by the previous selection procedure, we attained an indicator value for each set of traits at each site (Fig. 12). When adding up the traits identified as indicators for fumarole for each trait category and comparing them to the same sum value for Gabriel de Castilla samples (Fig. 12A–D), the samples collected at Fumarole Bay always presented significantly higher values. The same pattern was observed when a weighted mean of the trait sum indicators was applied by merging all the indicator categories (Fig. 12E). When applying the same procedure using the indicators selected by the point biserial correlation and PLS-DA-VIP analysis for the samples collected at Gabriel de Castilla station, the inverse trend was applied for both individual indicator traits (Fig. 12F–I) and the unified indicator index, merging all indicator categories (Fig. 12J). The samples collected near the GdC station exhibited significantly higher values.

4. Discussion

The preponderance of research directed towards metagenomic taxonomic and functional diversity in Deception Island centres on sediment microbial communities across various spatiotemporal and pressure gradients (Bendia et al., 2018; Centurion et al., 2021, 2022; Doytchinov and Dimov, 2022). Consequently, this study serves as a foundational exploration of prokaryotic and viral diversity and functions within this specific and extreme ecosystem. Consistent with previous studies, Proteobacteria, Bacteroidetes, and Actinobacteria were dominant in the Antarctic seawater (Liu and Jiang, 2020; Zhang et al., 2022). The site exhibiting heightened volcanic activity unsurprisingly presented a greater abundance of Archaea, known to flourish in seawater samples from locales with active volcanic activity, such as deep-sea hydrothermal systems (Takai et al., 2004), presumably owing to the distinctive environmental conditions conducive to microorganism growth (Huber et al., 2002). Euryarchaeota, specifically found in vent fluids from mid-ocean ridge subseafloor habitats (Huber et al., 2002) and waters surrounding deep-sea hydrothermal systems (Takai et al., 2004), adapt remarkably well to volcanic environments, particularly particle-rich coastal waters, and the specific temperature and chemical conditions (e.g., acidity) characterizing these areas (Curtis et al., 2013; Galand et al., 2008). Marine Euryarchaeota, which displays notable tolerance to Hg and the capacity to degrade various toxic heavy metals and xenobiotics (De and Ramaiah, 2007), supports this phylum's ability to contend with the elevated volcanic Hg concentrations in Fumarole Bay (Mão de Ferro et al., 2014). Several unique OTUs were observed in the samples from each sampling site, which were selected as potential indicator species. Nevertheless, a finer filter using the VIP score attained for the OTUs merged with the indicator species analysis statistics left the

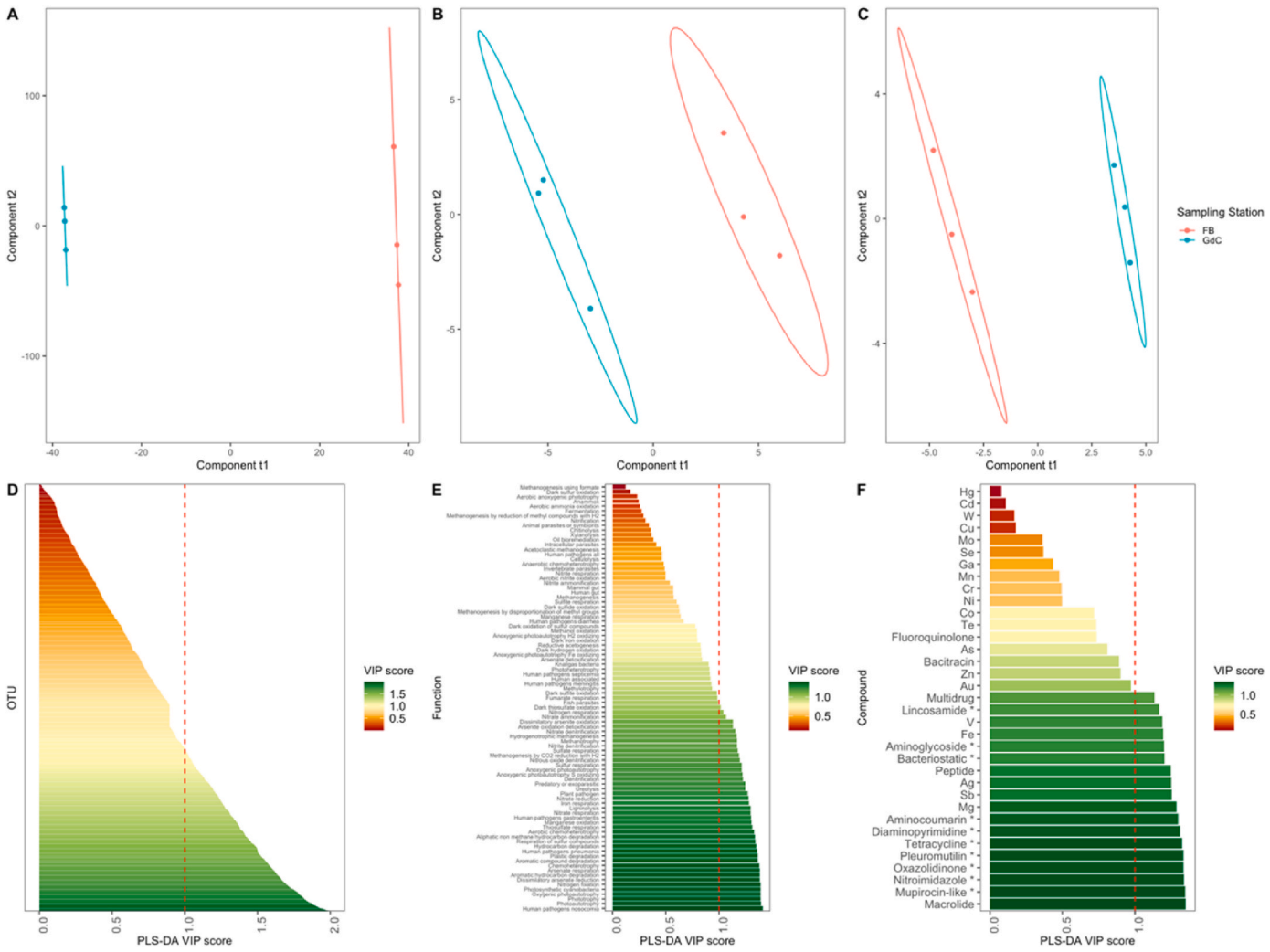

Fig. 10. Partial Least Square Discriminant Analysis (PLS-DA, A and B) and respective Variable Importance in Projection scores (PLS-DA VIP, C and D) of the taxonomic (A and C) and functional (B and D) traits of the water samples collected at the Fumarole Bay (FB) and Gabriel de Castilla (GdC) sampling sites (N = 3, dotted red line VIP = 1). (For interpretation of the references to color in this figure legend, the reader is referred to the Web version of this article.)

Euryarchaeota OTUs out of the biomarker OTUs sets assessed for each sampling site. This can be due to the known ubiquity of organisms belonging to Euryarchaeota, which allows them to cope and adapt to a variety of abiotic constraints (Flores et al., 2012). In the Bacteria kingdom, Actinobacteria, Cyanobacteria, Planctomycetes, and Synergistetes exhibited significantly higher abundance in Fumarole Bay samples. Actinobacteria, a major phylum in the domain Bacteria (Goodfellow and Fiedler, 2010), encompasses high GC-content Gram--positive bacteria from 17 different orders (Gao and Gupta, 2005; Sen et al., 2014). While the reasons remain unclear, prior studies have also noted a substantial abundance of Cyanobacteria in the hydrothermal system of Panarea Island as the dominant oxygenic phototrophs (Maugeri et al., 2013). The ability of certain Cyanobacteria to engage in diverse metabolic pathways, assimilating exogenous organic compounds (e.g., adenine, acetate, urea, leucine, uracil, and thymidine), underscores their ecological presence near hydrothermal vents (Colaço et al., 2006; Maugeri et al., 2013). Chemoautotrophic Planctomycetes and Synergistetes, which are highly abundant in metal-rich environments near hydrothermal vent fields (Stewart et al., 2018; Storesund et al., 2018), gain competitive advantage in these extreme environments (Colaço et al., 2006). The high abundance of marine Nucleocytoviricota, a group of large double-stranded DNA viruses, in volcanic vents and metal-rich environments, although in line with these areas' ability to boost ecosystem microbial diversity and activities, requires further exploration (Bortoluzzi et al., 2017; Price and Giovannelli, 2017). The presence of marine Fusobacteria and Bacteroidetes in coastal environments near human settlements in Antarctica stems from anthropogenic disturbances, notably the release of sewage from research stations, concomitant with high densities of fecal bacteria in these areas (Delille and Delille, 2000; Lo Giudice et al., 2019). Human activities serve as the primary source of marine Balneolaeota in Antarctic environments near human settlements (Lenihan, 1992, 1992, 1992; Lenihan et al., 1990). The presence of marine Ignavibacteriae in coastal environments near human settlements in Antarctica results from anthropogenic disturbances, including the release of contaminants, such as hydrocarbons, polychlorinated biphenyls, antibiotics, heavy metals, and (micro)plastics (Lo Giudice et al., 2019). Tenericutes bacteria, highly abundant in the glaciers near Gabriel de Castilla station (Garcia-Lopez et al., 2022), likely arise from glacier melting and water runoff in the coastal seawater area surrounding the Spanish station during the polar summer. These taxonomic variations suggest the potential utility of prokaryotic and viral ecological information as indicators of both human-induced disturbance and volcanic influence.

Submarine volcanic vents on Deception Island emit substantial quantities of metal sulfides (Angulo-Preckler et al., 2021), biotic methane (CH_4), and other hydrocarbons originating from microbial or thermogenic degradation of organic matter in sedimentary basins (Riedel et al., 2018; Rovere et al., 2022). These submarine volcanic vents

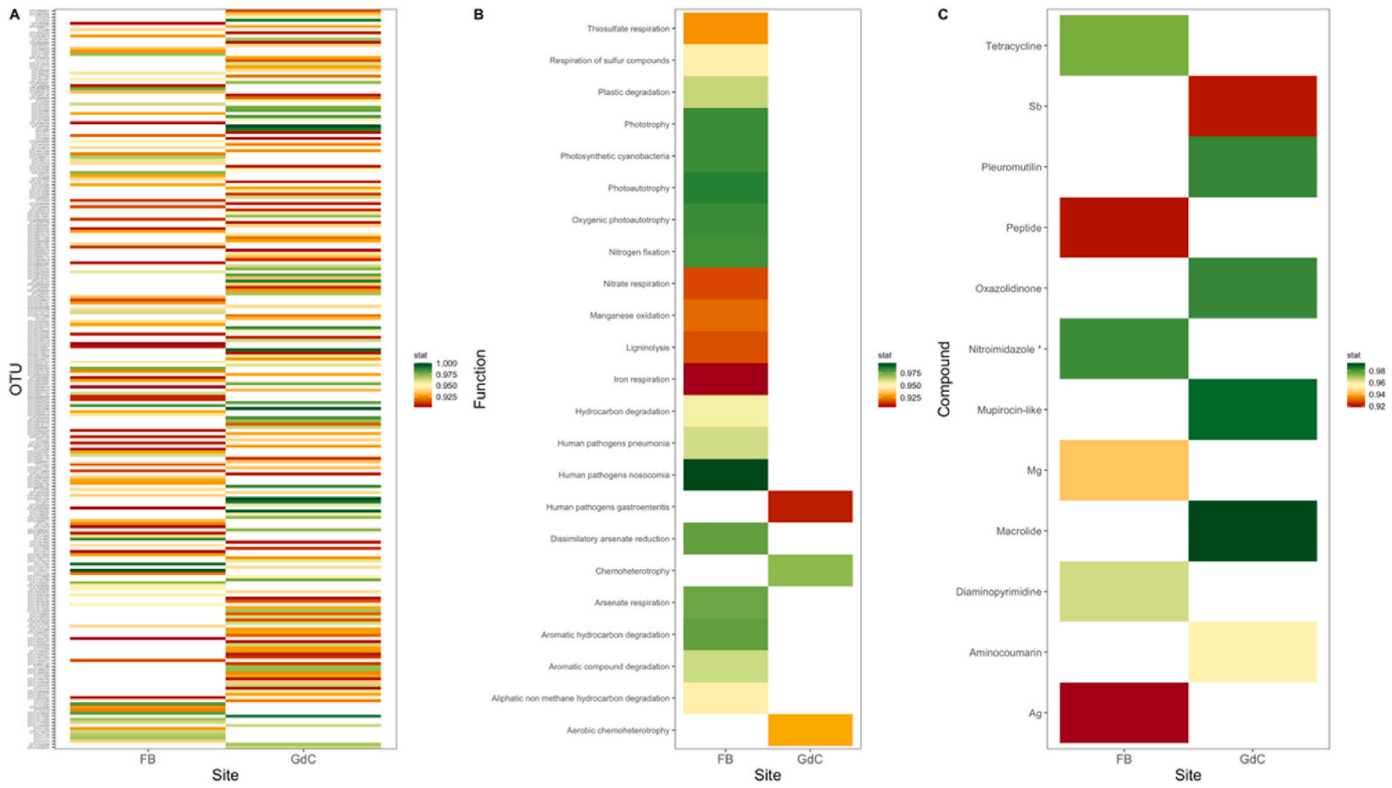

Fig. 11. Indicator species (A), putative metabolic functions (B), and resistome traits (C) point biserial correlation coefficient heat map of the water sample prokaryome and virome collected at the Fumarole Bay (FB) and Gabriel de Castilla (GdC) sampling sites (N = 3). Only indicators with a point biserial correlation coefficient higher than 0.90 and a Partial Least Square Discriminant Analysis Variable Importance in Projection scores higher than 1 were considered.

are also known to release various nutrients, including Fe, Si, P, and N, into seawater (González-Vega et al., 2020; Santana-Casiano et al., 2013). This substantiates not only a heightened prevalence of microorganisms with potential nitrogen metabolism-related functions, but also an augmented abundance of microbes with potential photoautotrophic functions in Fumarole Bay's communities, nourished by this substantial inorganic nutrient influx. The high abundance of Actinobacteria OTUs leads to an inevitable increase in organisms with potential pathogenic activity (mostly associated with nosocomial infections and pneumonia) in Fumarole Bay (Almasaudi, 2018; Hartzell et al., 2007). Conversely, in the vicinity of Gabriel de Castilla station, the increased abundance of pathogens associated with gastroenteritis is likely associated with wastewater outflow stemming from human settlements (Duarte et al., 2021b; Pertierra et al., 2014). The substantial input of dissolved organic matter from wastewater discharge creates an ideal environment for the growth of methanogenic prokaryotes (Qiao et al., 2015). Once again, as mentioned earlier for taxonomic traits, these distinctions in the potential functions of microorganisms already indicate certain functional attributes as potential indicators of human-induced disruption and volcanic impact.

Actinobacteria are recognized as significant producers of antibiotics and often demonstrate resistance to multiple drugs, contributing to the increased abundance and enrichment of antibiotic resistance genes (ARGs) (Su et al., 2015). The presence of these characteristics can be further intensified by the disposal of wastewater into Antarctic seawater, introducing non-indigenous bacteria and associated genetic elements (Stark et al., 2016) and affecting the bacterial community composition and ARG prevalence in Antarctic seawater (Zhang et al., 2022). In particular, in the study area, wastewater discharge from the Gabriel de Castilla base is likely due to a higher abundance of genes related to resistance against macrolide, bacteriostatic, aminocoumarin, multidrug, pleuromutilin, and mupirocin-like antibiotics in the vicinity of this human settlement (Duarte et al., 2021b). Previous studies (Fresia et al., 2019; Zhang et al., 2022) also indicated that the number of ARGs in low-impact areas is not necessarily lower than that in human-impacted aquatic environments. This suggests that the unique conditions in Fumarole Bay, influenced by active submarine volcanic activity, exert extreme selection pressure, fostering the development of specific ARGs (e.g., genes associated with resistance to tetracycline, aminoglycoside, peptide, nitroimidazole, diaminopyridine, and lincosamide-type antibiotics), possibly subject to horizontal transfer (Allen et al., 2010). Additionally, the submarine volcanic emissions of certain metal elements may have driven the selection of genes encoding both metal and antibiotic resistance (Baker-Austin et al., 2006). Despite the presence and persistence of these inorganic elements, conservation is expected not only in the vicinity of their emissions from volcanic cores but also throughout the entire bay. Unlike the organic molecules emitted by wastewater treatment plants, inorganic elements are present in the water column. The prolonged water residency time of the island bay, with a mean residence time of 2.4 years and only 1% volume exchange occurring per tidal cycle, contributes to a highly uniform concentration of these elements within the bay (Figueiredo et al., 2018; Mão de Ferro et al., 2013). This uniformity imparts a consistent selective pressure on the differential expression of metal resistance genes (MRGs), as evidenced by the lack of differences between the majority of MRG classes identified at both sites.

As outlined, certain taxonomic, functional, and resistance traits seem to be more closely associated with the inherent volcanic activity of the island, whereas other prokaryotic and viral community features appear to be more influenced by anthropogenic pressures in Deception Island Bay. In light of the imperative to address the impacts of human activities on the Antarctic ecosystem, particularly on Deception Island, it is crucial to identify potential indicator features capable of assessing the anthropogenic pressure conditions in the marine waters surrounding the island. Taxonomic and resistome features have proven effective in previous studies aimed at delineating various degrees of anthropogenic

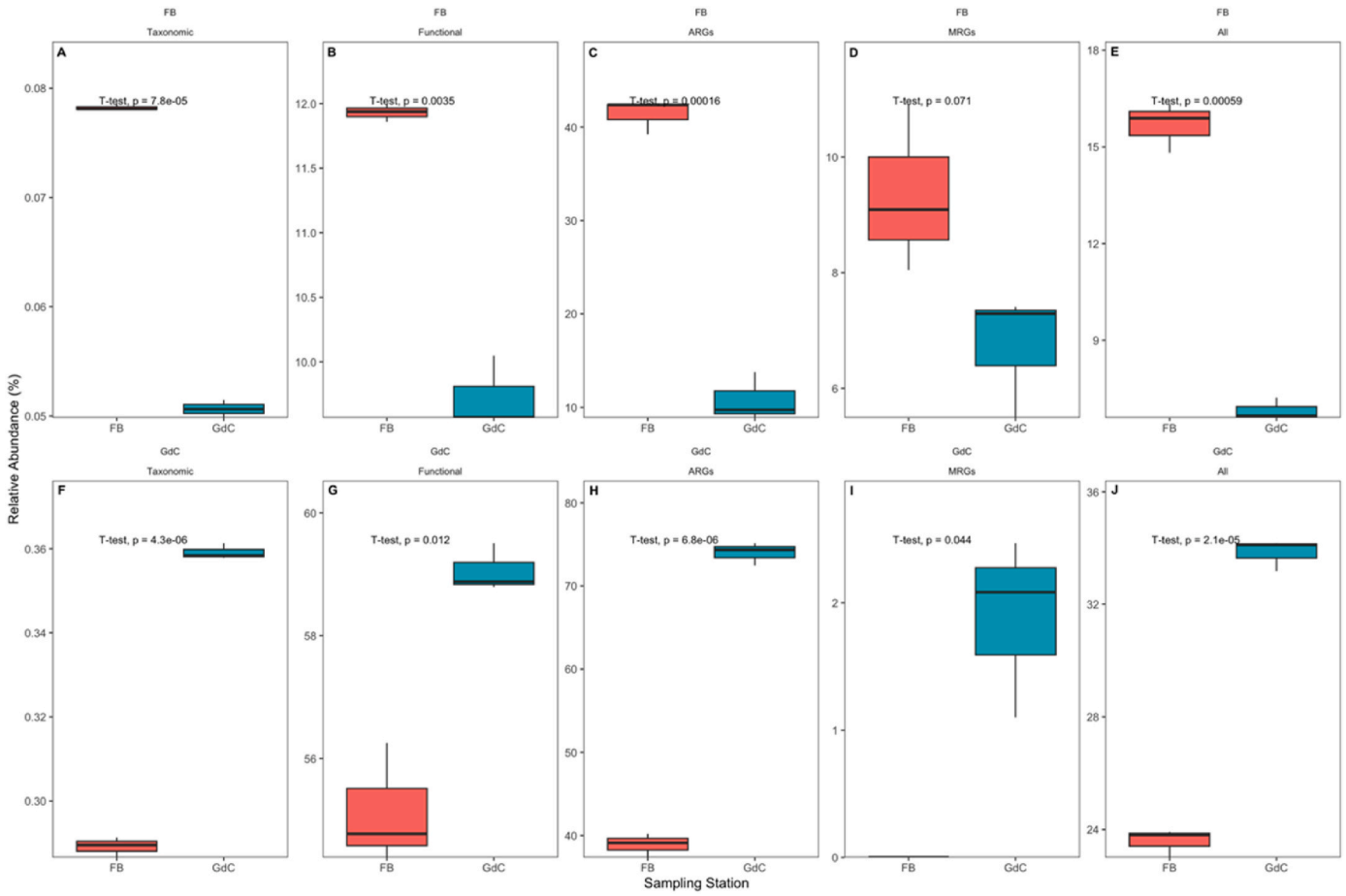

Fig. 12. Taxonomic, functional, and resistance indicator indices (sum of the indicator abundance) for Fumarole Bay (FB) (A–E) and Gabriel de Castilla (GdC) (F–J) sampling (N = 3) considering the indicators with a point biserial correlation coefficient higher than 0.90, and a Partial Least Square Discriminant Analysis Variable Importance in Projection scores higher than 1 were considered. The unified index (All) was calculated as the sum of the weighted (25%) value of each of the individual indices (*t*-test indicates the Student's t-test statistical significance value).

pressure in Atlantic systems, underscoring the potential applicability of such an approach to the marine ecosystems of Deception Island (Centurion et al., 2022; Duarte et al., 2022b). Four sets of site-specific indicators were derived by integrating two statistical methodologies to streamline the number of indicator features to a minimal yet acceptable quantity. The first selection of exclusive indicators for each site allowed for a reduction in the number of potential biomarkers for each site (831 and 851 for the samples collected at Gabriel de Castilla and Fumarole Bay, respectively). After submitting this high number of potential biomarker OTUs to a second filter using their importance in the PLS-DA projection, we were able to reduce the number of biomarker OTUs to 136 and 102 for Gabriel de Castilla and Fumarole Bay samples, respectively. The efficiency of these candidate biomarkers was further confirmed by analyzing their total abundance in the samples of the sites to which they were extracted and their site counterparts, revealing a high abundance always in the site to which they were compiled. This is of particular importance when dealing with large metagenomic datasets for indicator extraction, where the reduction achieved without discriminative power losses is of the utmost importance to allow a more streamlined analysis of the differences between sites with different pressures. Moreover, as mentioned above, the highlighted OTUs have a very direct relationship with the ecological function and resistome biomarkers, as well as with the conditions prevalent at each site, thus reinforcing the utility of the biomarker selection approach employed here. Although the ubiquity of several organisms and the proximity of the sampling sites within an enclosed island-bay system, the taxonomic functional and resistome traits here extracted as potential biomarkers of the abiotic differences known to be present at each site, are consistent with the literature available regarding not only the ecological traits of the selected OTUs, but also the pressure-response relationship known to shape functional and resistome traits, thus highlighting the accuracy and resolution of the biomarkers presented here.

5. Conclusions

Our investigation into metagenomic taxonomic, functional, and resistance traits in the marine ecosystems of Deception Island revealed intricate patterns influenced by both intrinsic volcanic activity and anthropogenic factors. The foundational understanding derived from the prevalent focus on sediment microbial communities highlights the dominance of specific bacterial and archaeal phyla in Antarctic seawater, with discernible variations attributed to volcanic and human-induced pressures. Adaptability of certain taxonomic groups (for example, Archaea) to withstand extreme conditions, and their role in coping with volcanic mercury concentrations, underscores their ecological prevalence. More cosmopolitan bacterial taxa also exhibited distinctive abundance patterns that are potentially linked to volcanic environments and hydrothermal systems. In terms of potential functional traits, notable specificities in Fumarole Bay were related to metal sulfide emissions from submarine volcanic vents and nutrient release, thus shaping functional diversity. Additionally, specific functions linked to potentially pathogenic microorganisms underscore the impact of anthropogenic activities on functional traits. Although resistance traits, particularly antibiotic resistance genes (ARGs), exhibited nuanced

patterns influenced by both anthropogenic pressures and volcanic activity, some could be related to wastewater disposal. To assess anthropogenic pressure, we proposed specific indicator features derived through statistical approaches as robust monitoring tools. The application of these indicator sets facilitated the differentiation of sampling areas based on their contrasting characteristics, rendering the data from both regions distinguishable. In the scenario of an increasing degree of anthropogenic pressure, exemplified by Fumarole Bay, it is anticipated that the set of indicators identified for Fumarole Bay would exhibit a reduction in abundance, approaching values similar to those assessed for the Gabriel de Castilla samples. Conversely, if measures are implemented to mitigate anthropogenic impacts in the vicinity of Gabriel de Castilla station, the abundance of selected indicator values for this area is expected to diminish and converge toward the values observed for Fumarole Bay. Consequently, the proposed set of indicator features has emerged as a promising monitoring tool capable of depicting different types (natural/volcanic and anthropogenic) and degrees of pressure in the marine waters of Deception Island. Overall, this study provides pivotal insights into the complex interplay of natural and anthropogenic factors shaping microbial communities and provides a basis for informed conservation and management strategies in the unique Antarctic ecosystem of Deception Island.

CRediT authorship contribution statement

Bernardo Duarte: Writing – original draft, Project administration, Data curation, Conceptualization. **Ana Cruz-Silva:** Writing – review & editing, Conceptualization. **Eduardo Feijão:** Writing – review & editing. **Marcelo Pereira:** Writing – review & editing, Data curation. **Mónica Nunes:** Writing – review & editing, Investigation. **Andreia Figueiredo:** Writing – review & editing. **Ana Rita Matos:** Writing – review & editing. **Ricardo Dias:** Writing – review & editing, Resources, Data curation. **Vanessa Fonseca:** Writing – review & editing, Formal analysis, Conceptualization. **Carla Gameiro:** Writing – review & editing, Project administration, Investigation. **Maria Teresa Cabrita:** Writing – review & editing, Project administration.

Declaration of competing interest

The authors declare that they have no known competing financial interests or personal relationships that could have appeared to influence the work reported in this paper.

Acknowledgments

The authors would like to thank Fundação para a Ciência e a Tecnologia (FCT) for funding MARE (Marine and Environmental Sciences Centre, http://doi.org/10.54499/UIDB/04292/2020 and http://doi.org/10.54499/UIDP/04292/2020), ARNET (Aquatic Research Network Associated Laboratory, http://doi.org/10.54499/LA/P/0069/2020), BioISI (Biosystems and Integrative Sciences Institute, http://doi.org/10.54499/UIDB/04046/2020 and http://doi.org/10.54499/UIDP/04046/2020), Ce3C (Centre for Ecology, Evolution and Environmental Changes, http://doi.org/10.54499/UIDB/00329/2020 and http://doi.org/10.54499/UIDP/00329/2020) and CHANGE (Global Change and Sustainability Institute, http://doi.org/10.54499/LA/P/0121/2020). The authors would also like to thank FCT, through the Portuguese Polar Program (PROPOLAR), for funding the Antarctic sampling campaigns, in this specific case through the Hg-Planktartic project. E. Feijão was supported by FCT Ph.D. Grant (2022.11260.BD). A. Cruz-Silva was funded by a fellowship from BioSys PhD program PD65-2012 (UI/BD/153050/2022). M.T. Cabrita was supported by a DL-57 research contract from Instituto de Geografia e Ordenamento do Território (IGOT). C. Gameiro was supported by a DL-57 research contract from Instituto from Instituto Português do Mar e Atmosfera (IPMA, I.P.) funded by the European Commission's Data Collection Framework, Mar2020 and Mar2030 under PNAB/EU-DCF - Programa Nacional de Amostragem Biológica/EU-Data Collection Framework (MAR-03.02.01-FEAMP-0015, MAR-03.02.01-FEAMP-0016 and MAR-014.7.2-FEAMPA-00001).

Appendix A. Supplementary data

Supplementary data to this article can be found online at https://doi.org/10.1016/j.indic.2024.100511.

Data availability

Data will be made available on request.

References

Allen, H.K., Donato, J., Wang, H.H., Cloud-Hansen, K.A., Davies, J., Handelsman, J., 2010. Call of the wild: antibiotic resistance genes in natural environments. Nat. Rev. Microbiol. 8, 251–259. https://doi.org/10.1038/nrmicro2312.

Almasaudi, S.B., 2018. Acinetobacter spp. as nosocomial pathogens: epidemiology and resistance features. Saudi J. Biol. Sci. 25, 586–596. https://doi.org/10.1016/j.sjbs.2016.02.009.

Amaro, E., Padeiro, A., Mão de Ferro, A., Mota, A.M., Leppe, M., Verkulich, S., Hughes, K.A., Peter, H.U., Canário, J., 2015. Assessing trace element contamination in fildes peninsula (King George Island) and ardley island, Antarctic. Mar. Pollut. Bull. 97, 523–527. https://doi.org/10.1016/j.marpolbul.2015.05.018.

Angulo-Preckler, C., Pernet, P., García-Hernández, C., Kereszturi, G., Álvarez-Valero, A. M., Hopfenblatt, J., Gómez-Ballesteros, M., Otero, X.L., Caza, J., Ruiz-Fernández, J., Geyer, A., Avila, C., 2021. Volcanism and rapid sedimentation affect the benthic communities of Deception Island, Antarctica. Continent. Shelf Res. 220, 104404. https://doi.org/10.1016/j.csr.2021.104404.

ARGs Desktop, 2023. A Cross-Platform Desktop Software for Antibiotic Resistance Genes Detection and Analysis from Metagenomic Data.

Arroyo-Rodríguez, V., Melo, F.P.L., Martínez-Ramos, M., Bongers, F., Chazdon, R.L., Meave, J.A., Norden, N., Santos, B.A., Leal, I.R., Tabarelli, M., 2017. Multiple successional pathways in human-modified tropical landscapes: new insights from forest succession, forest fragmentation and landscape ecology research. Biol. Rev. 92, 326–340. https://doi.org/10.1111/brv.12231.

Baker-Austin, C., Wright, M.S., Stepanauskas, R., McArthur, J.V., 2006. Co-selection of antibiotic and metal resistance. Trends Microbiol. 14, 176–182. https://doi.org/10.1016/j.tim.2006.02.006.

Baraldo, A., Rinaldi, C.A., 2000. Stratigraphy and structure of deception island, South Shetland islands, Antarctica. J. S. Am. Earth Sci. 13, 785–796. https://doi.org/10.1016/S0895-9811(00)00060-2.

Bargagli, R., 2008. Environmental contamination in Antarctic ecosystems. Sci. Total Environ. 400, 212–226. https://doi.org/10.1016/j.scitotenv.2008.06.062.

Bendia, A.G., Signori, C.N., Franco, D.C., Duarte, R.T.D., Bohannan, B.J.M., Pellizari, V. H., 2018. A mosaic of geothermal and marine features shapes microbial community structure on deception island volcano, Antarctica. Front. Microbiol. 9.

Bisht, S., Bargali, S.S., Bargali, K., Rawat, G.S., Rawat, Y.S., Fartyal, A., 2022. Influence of anthropogenic activities on forest carbon stocks—a case study from gori valley, western himalaya. Sustainability 14, 16918. https://doi.org/10.3390/su142416918.

Bisht, S., Bargali, S.S., Bargali, K., Rawat, Y.S., Rawat, G.S., 2023a. Dry matter dynamics and carbon flux along riverine forests of Gori valley, Western Himalaya. Front. For. Glob. Change 6. https://doi.org/10.3389/ffgc.2023.1206677.

Bisht, S., Rawat, G.S., Bargali, S.S., Rawat, Y.S., Mehta, A., 2023b. Forest vegetation response to anthropogenic pressures: a case study from Askot Wildlife Sanctuary, Western Himalaya. Environ. Dev. Sustain. 26, 10003–10027. https://doi.org/10.1007/s10668-023-03130-2.

Bortoluzzi, G., Romeo, T., La Cono, V., La Spada, G., Smedile, F., Esposito, V., Sabatino, G., Di Bella, M., Canese, S., Scotti, G., Bo, M., Giuliano, L., Jones, D., Golyshin, P.n., Yakimov, M.m., Andaloro, F., 2017. Ferrous iron- and ammonium-rich diffuse vents support habitat-specific communities in a shallow hydrothermal field off the Basiluzzo Islet (Aeolian Volcanic Archipelago). Geobiology 15, 664–677. https://doi.org/10.1111/gbi.12237.

Cáceres, M.D., Legendre, P., 2009. Associations between species and groups of sites: indices and statistical inference. Ecology 90, 3566–3574. https://doi.org/10.1890/08-1823.1.

Centurion, V., Silva, J., Duarte, A., Rosa, L., Oliveira, V., 2022. Comparing resistome profiles from anthropogenically impacted and non-impacted areas of two South Shetland Islands – maritime Antarctica. Environ. Pollut. 304, 119219. https://doi.org/10.1016/j.envpol.2022.119219.

Centurion, V.B., Campanaro, S., Basile, A., Treu, L., Oliveira, V.M., 2022. Microbiome structure in biofilms from a volcanic island in Maritime Antarctica investigated by genome-centric metagenomics and metatranscriptomics. Microbiol. Res. 265, 127197. https://doi.org/10.1016/j.micres.2022.127197.

Centurion, V.B., Lacerda-Júnior, G.V., Duarte, A.W.F., Silva, T.R., Silva, L.J., Rosa, L.H., Oliveira, V.M., 2021. Dynamics of microbial stress responses driven by abiotic changes along a temporal gradient in Deception Island, Maritime Antarctica. Sci. Total Environ. 758, 143671. https://doi.org/10.1016/j.scitotenv.2020.143671.

Chaturvedi, R.K., Raghubanshi, A.S., Singh, J.S., 2017. Sapling harvest: a predominant factor affecting future composition of tropical dry forests. For. Ecol. Manag. 384, 221–235. https://doi.org/10.1016/j.foreco.2016.10.026.

Chen, J., Cui, Y., Xiao, Q., Lin, K., Wang, B., Zhou, J., Li, X., 2024. Difference in microbial community structure along a gradient of crater altitude: insights from the Nushan volcano. Appl. Environ. Microbiol. 90, e00753. https://doi.org/10.1128/aem.00753-24, 24.

Colaço, A., Raghukumar, C., Mohandass, C., Cardigos, F., Santos, R.S., 2006. Effect of shallow-waterventing in Azores on a few marine biota. Cah. Biol. Mar. 47, 359–364.

COMNAP, 2017. Antarctic Station Catalogue. Council of Managers of National Antarctic Programs.

Curtis, A.C., Wheat, C.G., Fryer, P., Moyer, C.L., 2013. Mariana forearc Serpentinite Mud Volcanoes Harbor novel communities of extremophilic Archaea. Geomicrobiol. J. 30, 430–441. https://doi.org/10.1080/01490451.2012.705226.

De, J., Ramaiah, N., 2007. Characterization of marine bacteria highly resistant to mercury exhibiting multiple resistances to toxic chemicals. Ecol. Indicat. 7, 511–520. https://doi.org/10.1016/j.ecolind.2006.05.002.

Delille, D., Delille, E., 2000. Distribution of enteric bacteria in antarctic seawater surrounding the dumont d'Urville permanent station (Adélie Land). Mar. Pollut. Bull. 40, 869–872. https://doi.org/10.1016/S0025-326X(00)00077-1.

Dhariwal, A., Junges, R., Chen, T., Petersen, F.C., 2021. ResistoXplorer: a web-based tool for visual, statistical and exploratory data analysis of resistome data. NAR Genomics Bioinform. 3, lqab018. https://doi.org/10.1093/nargab/lqab018.

Dibbern, J.S., 2010. Fur seals, whales and tourists: a commercial history of Deception Island, Antarctica. Polar Rec. 46, 210–221. https://doi.org/10.1017/S0032247409008651.

Doytchinov, V.V., Dimov, S.G., 2022. Microbial community composition of the antarctic ecosystems: review of the bacteria, fungi, and Archaea identified through an NGS-based metagenomics approach. Life 12, 916. https://doi.org/10.3390/life12060916.

Duarte, B., Cabrita, M.T., Vidal, T., Pereira, J.L., Pacheco, M., Pereira, P., Canário, J., Gonçalves, F.J.M., Matos, A.R., Rosa, R., Marques, J.C., Caçador, I., Gameiro, C., 2018. Phytoplankton community-level bio-optical assessment in a naturally mercury contaminated Antarctic ecosystem (Deception Island). Mar. Environ. Res. 140, 412–421. https://doi.org/10.1016/j.marenvres.2018.07.014.

Duarte, B., Feijão, E., Cruz de Carvalho, R., Duarte, I.A., Marques, A.P., Maia, M., Hertzog, J., Matos, A.R., Cabrita, M.T., Caçador, I., Figueiredo, A., Silva, M.S., Cordeiro, C., Fonseca, V.F., 2022a. Untargeted metabolomics reveals antidepressant effects in a marine photosynthetic organism: the diatom phaeodactylum tricornutum as a case study. Biology 11. https://doi.org/10.3390/biology11121770.

Duarte, B., Feijão, E., Cruz de Carvalho, R., Franzitta, M., Carlos Marques, J., Caçador, I., Teresa Cabrita, M., Fonseca, V.F., 2021a. Unlocking Kautsky's dark box: development of an optical toxicity classification tool (OPTOX index) with marine diatoms exposed to emerging contaminants. Ecol. Indicat. 131, 108238. https://doi.org/10.1016/j.ecolind.2021.108238.

Duarte, B., Figueiredo, A., Ramalhosa, P., Canning-Clode, J., Caçador, I., Fonseca, V.F., 2022b. Unravelling the Portuguese coastal and transitional waters' microbial resistome as a biomarker of differential anthropogenic impact. Toxics 10. https://doi.org/10.3390/toxics10100613.

Duarte, B., Gameiro, C., Matos, A.R., Figueiredo, A., Silva, M.S., Cordeiro, C., Caçador, I., Reis-Santos, P., Fonseca, V., Cabrita, M.T., 2021b. First screening of biocides, persistent organic pollutants, pharmaceutical and personal care products in Antarctic phytoplankton from Deception Island by FT-ICR-MS. Chemosphere 274, 129860. https://doi.org/10.1016/j.chemosphere.2021.129860.

Duarte, I.A., Reis-Santos, P., Novais, S.C., Rato, L.D., Lemos, M.F.L.L., Freitas, A., Pouca, A.S.V., Barbosa, J., Cabral, H.N., Fonseca, V.F., 2020. Depressed, hypertense and sore: long-term effects of fluoxetine, propranolol and diclofenac exposure in a top predator fish. Sci. Total Environ. 712. https://doi.org/10.1016/j.scitotenv.2020.136564.

Emnet, P., Gaw, S., Northcott, G., Storey, B., Graham, L., 2015. Personal care products and steroid hormones in the Antarctic coastal environment associated with two Antarctic research stations, McMurdo Station and Scott Base. Environ. Res. 136, 331–342. https://doi.org/10.1016/j.envres.2014.10.019.

Esteban, S., Moreno-Merino, L., Matellanes, R., Catalá, M., Gorga, M., Petrovic, M., López de Alda, M., Barceló, D., Durán, J.J., López-Martínez, J., Valcárcel, Y., Valcárcel, Y., 2016. Presence of endocrine disruptors in freshwater in the northern Antarctic Peninsula region. Environ. Res. 147, 179–192. https://doi.org/10.1016/j.envres.2016.01.034.

Ewbank, A.C., Esperón, F., Sacristán, C., Sacristán, I., Krul, R., Cavalcante de Macedo, E., Calatayud, O., Bueno, I., de Francisco Strefezzi, R., Catão-Dias, J.L., 2021. Seabirds as anthropization indicators in two different tropical biotopes: a One Health approach to the issue of antimicrobial resistance genes pollution in oceanic islands. Sci. Total Environ. 754, 142141. https://doi.org/10.1016/j.scitotenv.2020.142141.

Figueiredo, D., Dos Santos, A., Mateus, M., Pinto, L., 2018. Hydrodynamic modelling of Port foster, deception island, Antarctica. Antarct. Sci. 30, 115–124. https://doi.org/10.1017/S0954102017000463.

Flores, G.E., Wagner, I.D., Liu, Y., Reysenbach, A.-L., 2012. Distribution, abundance, and diversity patterns of the thermoacidophilic "deep-sea hydrothermal vent Euryarchaeota 2.". Front. Microbiol. 3. https://doi.org/10.3389/fmicb.2012.00047.

Fonseca, V.F., Duarte, I.A., Duarte, B., Freitas, A., Pouca, A.S.V., Barbosa, J., Gillanders, B.M., Reis-Santos, P., 2021. Environmental risk assessment and bioaccumulation of pharmaceuticals in a large urbanized estuary. Sci. Total Environ. 783. https://doi.org/10.1016/j.scitotenv.2021.147021.

Foster, Z.S.L., Sharpton, T.J., Grünwald, N.J., 2017. Metacoder: an R package for visualization and manipulation of community taxonomic diversity data. PLoS Comput. Biol. 13, e1005404. https://doi.org/10.1371/journal.pcbi.1005404.

Fresia, P., Antelo, V., Salazar, C., Giménez, M., D'Alessandro, B., Afshinnekoo, E., Mason, C., Gonnet, G.H., Iraola, G., 2019. Urban metagenomics uncover antibiotic resistance reservoirs in coastal beach and sewage waters. Microbiome 7, 35. https://doi.org/10.1186/s40168-019-0648-z.

Galand, P.E., Lovejoy, C., Pouliot, J., Vincent, W.F., 2008. Heterogeneous archaeal communities in the particle-rich environment of an arctic shelf ecosystem. J. Marine Sys. Sea ice and life in a river-influenced arctic shelf ecosystem 74, 774–782. https://doi.org/10.1016/j.jmarsys.2007.12.001.

Gao, B., Gupta, R.S., 2005. Conserved indels in protein sequences that are characteristic of the phylum Actinobacteria. Int. J. Syst. Evol. Microbiol. 55, 2401–2412. https://doi.org/10.1099/ijs.0.63785-0.

Garcia-Lopez, E., Ruiz-Blas, F., Sanchez-Casanova, S., Peña Perez, S., Martin-Cerezo, M. L., Cid, C., 2022. Microbial communities in volcanic glacier ecosystems. Front. Microbiol. 13.

González-Vega, A., Fraile-Nuez, E., Santana-Casiano, J.M., González-Dávila, M., Escánez-Pérez, J., Gómez-Ballesteros, M., Tello, O., Arrieta, J.M., 2020. Significant release of dissolved inorganic nutrients from the shallow submarine volcano tagoro (Canary Islands) based on seven-year monitoring. Front. Mar. Sci. 6.

Goodfellow, M., Fiedler, H.-P., 2010. A guide to successful bioprospecting: informed by actinobacterial systematics. Antonie Leeuwenhoek 98, 119–142. https://doi.org/10.1007/s10482-010-9460-2.

Gunnarsdóttir, R., Jenssen, P.D., Erland Jensen, P., Villumsen, A., Kallenborn, R., 2013. A review of wastewater handling in the Arctic with special reference to pharmaceuticals and personal care products (PPCPs) and microbial pollution. Ecol. Eng. 50, 76–85. https://doi.org/10.1016/j.ecoleng.2012.04.025.

Hartzell, J.D., Kim, A.S., Kortepeter, M.G., Moran, K.A., 2007. Acinetobacter pneumonia: a review. MedGenMed 9, 4.

Huber, J.A., Butterfield, D.A., Baross, J.A., 2002. Temporal changes in archaeal diversity and chemistry in a mid-ocean ridge subseafloor habitat. Appl. Environ. Microbiol. 68, 1585–1594. https://doi.org/10.1128/AEM.68.4.1585-1594.2002.

IAATO, 2017. IAATO (International Association of Antarctica Tour Operators) statis-tics [WWW Document]. In: 2016-2017 Number Tour. Visit. Per Site/per Act. - Sorted by All Sites, Cont. Penins. URL. www.iaato.org. (Accessed 1 July 2024).

Jardine, J., Mavumengwana, V., Ubomba-Jaswa, E., 2019. Antibiotic resistance and heavy metal tolerance in cultured bacteria from hot springs as indicators of environmental intrinsic resistance and tolerance levels. Environ. Pollut. 249, 696–702. https://doi.org/10.1016/j.envpol.2019.03.059.

Kassambara, A., 2023. Ggpubr: "Ggplot2" Based Publication Ready Plots.

Lenihan, H.S., 1992. Benthic marine pollution around McMurdo station, Antarctica: a summary of findings. Marine pollution bulletin, environmental awareness in Antarctica: history, problems, and. Future Solut. 25, 318–323. https://doi.org/10.1016/0025-326X(92)90689-4.

Lenihan, H.S., Oliver, J.S., Oakden, J.M., Stephenson, M.D., 1990. Intense and localized benthic marine pollution around McMurdo Station, Antarctica. Mar. Pollut. Bull. 21, 422–430. https://doi.org/10.1016/0025-326X(90)90761-V.

Lenn, Y.D., Chereskin, T.K., Glatts, R.C., 2003. Seasonal to tidal variability in currents, stratification and acoustic backscatter in an Antarctic ecosystem at Deception Island. Deep-Sea Res. Part II Top. Stud. Oceanogr. 50, 1665–1683. https://doi.org/10.1016/S0967-0645(03)00085-7.

Liu, C., Cui, Y., Li, X., Yao, M., 2021. microeco: an R package for data mining in microbial community ecology. FEMS (Fed. Eur. Microbiol. Soc.) Microbiol. Ecol. 97, fiaa255. https://doi.org/10.1093/femsec/fiaa255.

Liu, Q., Jiang, Y., 2020. Application of microbial network analysis to discriminate environmental heterogeneity in Fildes Peninsula, Antarctica. Mar. Pollut. Bull. 156, 111244. https://doi.org/10.1016/j.marpolbul.2020.111244.

Lo Giudice, A., Caruso, G., Rizzo, C., Papale, M., Azzaro, M., 2019. Bacterial communities versus anthropogenic disturbances in the Antarctic coastal marine environment. Environ. Sustain. 2, 297–310. https://doi.org/10.1007/s42398-019-00064-2.

Louca, S., Parfrey, L.W., Doebeli, M., 2016. Decoupling function and taxonomy in the global ocean microbiome. Science 353, 1272–1277. https://doi.org/10.1126/science.aaf4507.

Maletha, A., Maikhuri, R.K., Bargali, S.S., 2023. Population structure and regeneration pattern of himalayan birch (Betula utilis D.Don) in the timberline zone of Nanda Devi Biosphere Reserve, western himalaya, India. Geology, Ecology, and Landscapes 7, 248–257. https://doi.org/10.1080/24749508.2021.1952767.

Maletha, A., Maikhuri, R.K., Bargali, S.S., 2020. Criteria and indicator for assessing threat on Himalayan birch (B. utilis) at timberline ecotone of Nanda Devi Biosphere Reserve: a world heritage site, Western Himalaya, India. Environ. Sustain. Indicators 8, 100086. https://doi.org/10.1016/j.indic.2020.100086.

Mão de Ferro, A., Mota, A.M., Canário, J., Ferro, A.M.D., Mota, A.M., Canário, J., 2013. Sources and transport of As, Cu, Cd and Pb in the environmental compartments of Deception Island, Antarctica. Mar. Pollut. Bull. 77, 341–348. https://doi.org/10.1016/j.marpolbul.2013.08.037.

Mão de Ferro, A., Mota, A.M., Canário, J., Ferro, A.M.D., Mota, A.M., Canário, J., Mão de Ferro, A., Mota, A.M., Canário, J., 2014. Pathways and speciation of mercury in the environmental compartments of Deception Island, Antarctica. Chemosphere 95, 227–233. https://doi.org/10.1016/j.chemosphere.2013.08.081.

Maugeri, T.L., Lentini, V., Spanò, A., Gugliandolo, C., 2013. Abundance and diversity of picocyanobacteria in shallow hydrothermal vents of Panarea island (Italy). Geomicrobiol. J. 30, 93–99. https://doi.org/10.1080/01490451.2011.653088.

McClelland, R., 2011. Ground Layer Response to Disturbance in the Pine-Dominated Eastern Foothill Region of West- Central Alberta, Canada (PhD Thesis). Southern Illinois University Carbondale.

McMurdie, P.J., Holmes, S., 2013. Phyloseq: an R package for reproducible interactive analysis and graphics of microbiome census data. PLoS One 8, e61217. https://doi.org/10.1371/journal.pone.0061217.

Naveen, R., Lynch, H.J., Forrest, S., Mueller, T., Polito, M., 2012. First direct, site-wide penguin survey at Deception Island, Antarctica, suggests significant declines in breeding chinstrap penguins. Polar Biol. 35, 1879–1888. https://doi.org/10.1007/s00300-012-1230-3.

Padeiro, A., Amaro, E., Correia Dos Santos, M.M., Araújo, M.F., Gomes, S.S., Leppe, M., Verkulich, S., Hughes, K.A., Peter, H.-U., Canário, J., 2016. Trace element contamination and availability in fildes peninsula, king george island, Antarctica. Environ. Sci. J. Integr. Environ. Res.: Process. Impacts 18, 648–657. https://doi.org/10.1039/C6EM00052E.

Pal, C., Bengtsson-Palme, J., Rensing, C., Kristiansson, E., Larsson, D.G.J., 2014. BacMet: antibacterial biocide and metal resistance genes database. Nucleic Acids Res. 42, D737–D743. https://doi.org/10.1093/nar/gkt1252.

Pertierra, L.R., Tejedo, P., Benayas, J., 2014. Historical developments, drivers of change and future scenarios for human activities on deception island. In: Tin, T., Liggett, D., Maher, P.T., Lamers, M. (Eds.), Antarctic Futures: Human Engagement with the Antarctic Environment. Springer, Netherlands, Dordrecht, pp. 193–211. https://doi.org/10.1007/978-94-007-6582-5_8.

Price, R.E., Giovannelli, D., 2017. A review of the geochemistry and microbiology of marine shallow-water hydrothermal vents. In: Reference Module in Earth Systems and Environmental Sciences. Elsevier. https://doi.org/10.1016/B978-0-12-409548-9.09523-3.

Qiao, S., Tian, T., Qi, B., Zhou, J., 2015. Methanogenesis from wastewater stimulated by addition of elemental manganese. Sci. Rep. 5, 12732. https://doi.org/10.1038/srep12732.

Rey, J., Somoza, L., Martínez-Frías, J., 1995. Tectonic, volcanic, and hydrothermal event sequence on Deception Island (Antarctica). Geo Mar. Lett. 15, 1–8. https://doi.org/10.1007/BF01204491.

Riedel, M., Scherwath, M., Römer, M., Veloso, M., Heesemann, M., Spence, G.D., 2018. Distributed natural gas venting offshore along the Cascadia margin. Nat. Commun. 9, 3264. https://doi.org/10.1038/s41467-018-05736-x.

Rovere, M., Mercorella, A., Gamberi, F., Zgur, F., 2022. Hydrothermal vent complexes control seepage and hydrocarbon release on the overriding plate of the tyrrhenian-ionian subduction system (Paola basin). Front. Earth Sci. 10.

Sanchez, G., 2013. Package 'DiscriMiner'.

Santana-Casiano, J.M., González-Dávila, M., Fraile-Nuez, E., de Armas, D., González, A. G., Domínguez-Yanes, J.F., Escánez, J., 2013. The natural ocean acidification and fertilization event caused by the submarine eruption of El Hierro. Sci. Rep. 3, 1140. https://doi.org/10.1038/srep01140.

Santos, A., Burgos, F., Martinez-Urtaza, J., Barrientos, L., 2022. Metagenomic Characterization of resistance genes in deception island and their association with mobile genetic elements. Microorganisms 10, 1432. https://doi.org/10.3390/microorganisms10071432.

Schmieder, R., Edwards, R., 2011. Quality control and preprocessing of metagenomic datasets. Bioinformatics 27, 863–864. https://doi.org/10.1093/bioinformatics/btr026.

Sen, A., Daubin, V., Abrouk, D., Gifford, I., Berry, A.M., Normand, P., 2014. Phylogeny of the class Actinobacteria revisited in the light of complete genomes. The orders 'Frankiales' and Micrococcales should be split into coherent entities: proposal of Frankiales ord. nov., Geodermatophilales ord. nov., Acidothermales ord. nov. and Nakamurellales ord. nov. Int. J. Syst. Evol. Microbiol. 64, 3821–3832. https://doi.org/10.1099/ijs.0.063966-0.

Stark, J.S., Corbett, P.A., Dunshea, G., Johnstone, G., King, C., Mondon, J.A., Power, M. L., Samuel, A., Snape, I., Riddle, M., 2016. The environmental impact of sewage and wastewater outfalls in Antarctica: an example from Davis station, East Antarctica. Water Res. 105, 602–614. https://doi.org/10.1016/j.watres.2016.09.026.

Stewart, L.C., Stucker, V.K., Stott, M.B., de Ronde, C.E.J., 2018. Marine-influenced microbial communities inhabit terrestrial hot springs on a remote island volcano. Extremophiles 22, 687–698. https://doi.org/10.1007/s00792-018-1029-4.

Storesund, J.E., Lanzèn, A., García-Moyano, A., Reysenbach, A.-L., Øvreås, L., 2018. Diversity patterns and isolation of Planctomycetes associated with metalliferous deposits from hydrothermal vent fields along the Valu Fa Ridge (SW Pacific). Antonie Leeuwenhoek 111, 841–858. https://doi.org/10.1007/s10482-018-1026-8.

Su, J.-Q., Wei, B., Ou-Yang, W.-Y., Huang, F.-Y., Zhao, Y., Xu, H.-J., Zhu, Y.-G., 2015. Antibiotic resistome and its association with bacterial communities during sewage sludge composting. Environ. Sci. Technol. 49, 7356–7363. https://doi.org/10.1021/acs.est.5b01012.

Takai, K., Oida, H., Suzuki, Y., Hirayama, H., Nakagawa, S., Nunoura, T., Inagaki, F., Nealson, K.H., Horikoshi, K., 2004. Spatial distribution of marine Crenarchaeota group I in the vicinity of deep-sea hydrothermal systems. Appl. Environ. Microbiol. 70, 2404–2413. https://doi.org/10.1128/AEM.70.4.2404-2413.2004.

Thomaidis, N.S., Asimakopoulos, A.G., Bletsou, A.A., 2012. Emerging contaminants: a tutorial mini-review. Global Nest J. 14, 72–79.

Wood, D.E., Lu, J., Langmead, B., 2019. Improved metagenomic analysis with Kraken 2. Genome Biol. 20, 257. https://doi.org/10.1186/s13059-019-1891-0.

Zhang, T., Ji, Z., Li, J., Yu, L., 2022. Metagenomic insights into the antibiotic resistome in freshwater and seawater from an Antarctic ice-free area. Environ. Pollut. 309, 119738. https://doi.org/10.1016/j.envpol.2022.119738.